iScience

CellPress
OPEN ACCESS

Article

Tet controls axon guidance in early brain development through glutamatergic signaling

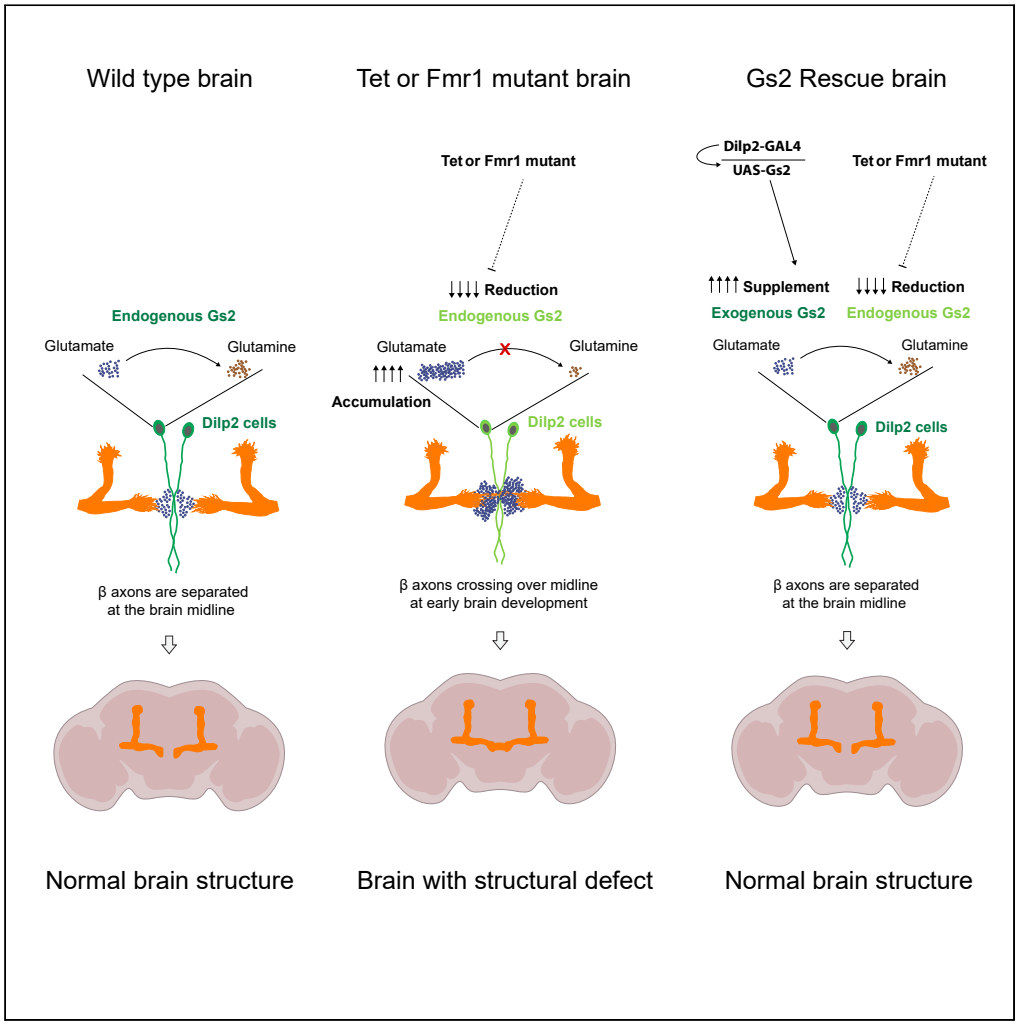

Hiep Tran, Le Le, Badri Nath Singh, Joseph Kramer, Ruth Steward

steward@waksman.rutgers.edu

Highlights

Tet controls axon guidance at early brain development through its DNA-binding domain

Tet regulates glutamatergic signaling by controlling the expression levels of Gs2

Tet and Gs2 are required in the insulin-producing cells (IPCs)

Overexpression of Gs2 in the IPCs can rescue axonal defects in Tet and Fmr1 mutants

Tran et al., iScience 27, 109634
May 17, 2024 © 2024 Published by Elsevier Inc.
https://doi.org/10.1016/j.isci.2024.109634

iScience

CellPress
OPEN ACCESS

Article

Tet controls axon guidance in early brain development through glutamatergic signaling

Hiep Tran,[1] Le Le,[1] Badri Nath Singh,[1] Joseph Kramer,[3] and Ruth Steward[1,2,4,*]

SUMMARY

Mutations in ten-eleven translocation (TET) proteins are associated with human neurodevelopmental disorders. We find a function of Tet in regulating *Drosophila* early brain development. The Tet DNA-binding domain (Tet^{AXXC}) is required for axon guidance in the mushroom body (MB). Glutamine synthetase 2 (Gs2), a key enzyme in glutamatergic signaling, is significantly down-regulated in the Tet^{AXXC} brains. Loss of Gs2 recapitulates the Tet^{AXXC} phenotype. Surprisingly, Tet and Gs2 act in the insulin-producing cells (IPCs) to control MB axon guidance, and overexpression of Gs2 in IPCs rescues the defects of Tet^{AXXC}. Feeding Tet^{AXXC} with metabotropic glutamate receptor antagonist MPEP rescues the phenotype while glutamate enhances it. Mutants in Tet and *Drosophila* Fmr1, the homolog of human FMR1, have similar defects, and overexpression of Gs2 in IPCs also rescues the Fmr1 phenotype. We provide the first evidence that Tet controls the guidance of developing brain axons by modulating glutamatergic signaling.

INTRODUCTION

Ten-eleven translocation (TET) is one of the most important epigenetic and epi-transcriptomic regulators. TET can regulate DNA methylation in the genome as well as RNA hydroxymethylation through its catalytic activity.[1–4] TET is an essential gene for animal development. Loss of all three TET genes in mice leads to embryonic lethality.[5] *Drosophila* has one highly conserved Tet homolog and the Tet^{null} mutant dies at the late pupal stage.[6] Mammalian TETs are expressed in various tissues while *Drosophila* Tet is highly expressed in neuronal tissues including the brain.[6,7] Recently, TET mutations in humans have been linked to neurodevelopmental disorders (NDs) associated with intellectual disability and autism spectrum disorders.[8–11] One key process during brain development is axon guidance and the mis-regulation of axon guidance can lead to neurodevelopmental disorders.[12] To test whether Tet functions in axon guidance, we used a well-studied axonal structure in the *Drosophila* brain, the mushroom body (MB).

The insect MB is the analogous structure of the human hippocampus.[13] In *Drosophila*, the MB is responsible for learning, memory, circadian rhythms, sleep, and courtship.[14,15] In each brain hemisphere, the MB structure develops from four embryonic MB neuroblasts.[16] During the development, these MB neuroblasts sequentially generate different classes of MB neurons whose axons bundle into γ, α′/β′, and α/β lobes.[16] These MB lobes can be divided into 15 compartments which are connected to specific MB output neurons or dopaminergic neurons as part of the brain circuit to modulate a variety of brain functions.[14] Thus, MB axon guidance is highly regulated to ensure proper brain circuitry.

Glutamatergic signaling is the major excitatory pathway in the brain and has key roles in neuronal plasticity, development, learning, and memory.[17–19] The NMDA-type glutamate receptors (NMDARs) are present in axons and growth cones of young hippocampal neurons.[20] Mis-regulation of the glutamate metabotropic receptor (mGluR) signaling causes neuronal defects.[21] Glutamate levels can affect the growth rate and branching of dopaminergic neurons *in vitro*.[22] In addition, the responsiveness of growth cones to repellent molecules such as slit-2, semaphoring 3A, and semaphoring 3C is dependent on the levels of glutamate in the growth cone culture medium.[23] However, there is limited *in vivo* evidence on whether and how glutamatergic signaling can control axon guidance.

Fragile X messenger ribonucleoprotein 1 (FMR1) is a human gene that is important for regulating synaptic plasticity, protein synthesis, and dendritic morphology.[24] In patients with fragile X syndrome (FXS), the most common form of inherited intellectual and developmental disability, the gene generally is silenced by CGG trinucleotide expansion in the promoter region.[24] FMR1 is conserved in *Drosophila* and mutants in the *Fmr1* homolog have been used to study the requirement of the gene and to identify potential therapeutic treatments for FXS.[25,26] The *Drosophila Fmr1* mutants have been shown to have defects in axon guidance and to affect neurological functions such as learning and memory as well as courtship behavior.[21,27]

In this study, we investigate a new function of *Tet* in brain development. We found that Tet controls MB axon guidance by regulating glutamine synthetase 2 (Gs2), a key enzyme in glutamatergic signaling. Site-specific mutations allowed us to determine that the Tet DNA-binding

[1]Waksman Institute, Rutgers University, Piscataway, NJ 08854, USA
[2]Department of Molecular Biology and Biochemistry, Cancer Institute of New Jersey, Rutgers University, New Brunswick, NJ 08901, USA
[3]Department of Pathology and Laboratory Medicine, Rutgers Biomedical and Health Sciences, Rutgers University, New Brunswick, NJ 08901, USA
[4]Lead contact
*Correspondence: steward@waksman.rutgers.edu
https://doi.org/10.1016/j.isci.2024.109634

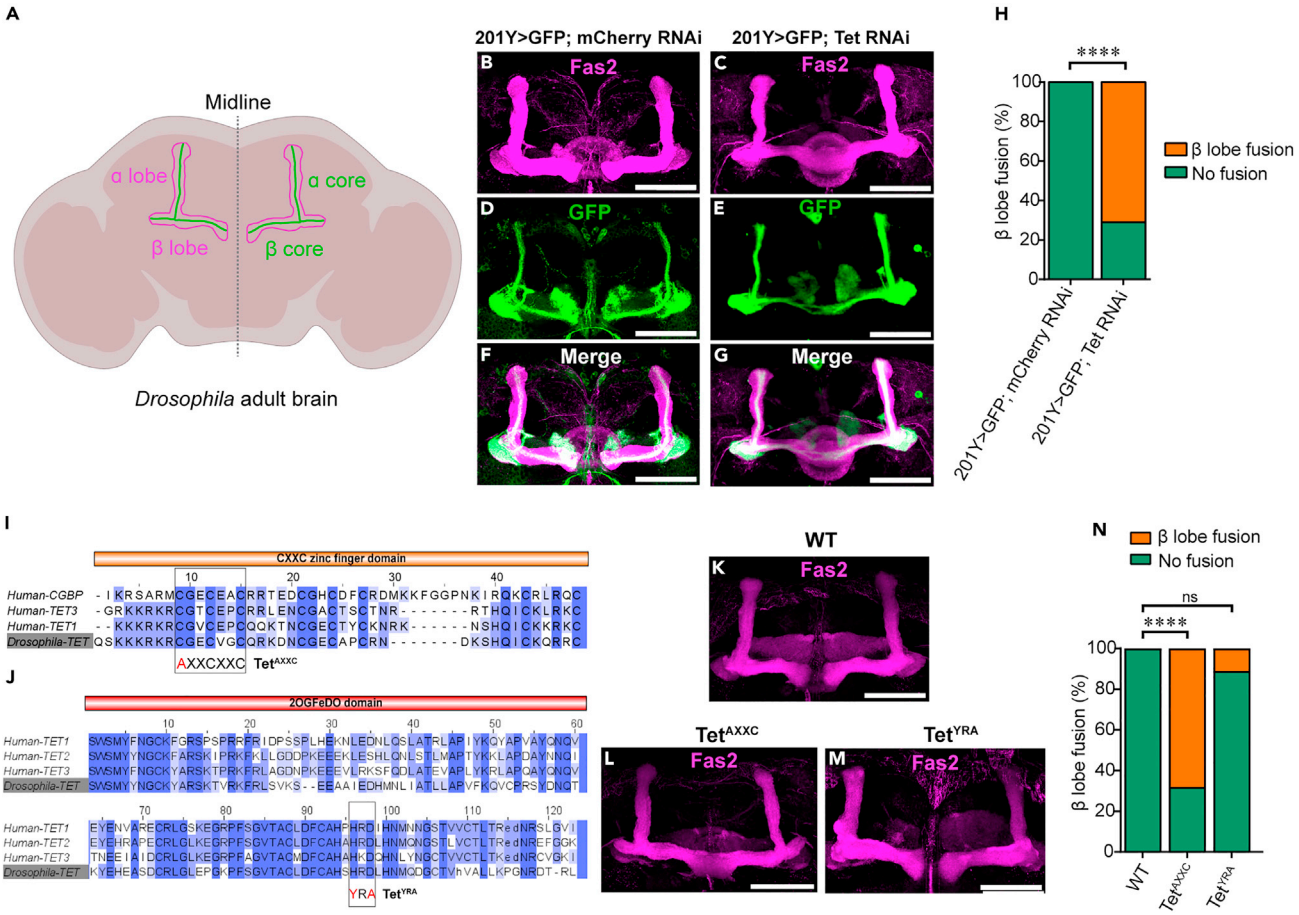

Figure 1. Tet and its DNA-binding domain are required for proper MB β axon guidance

(A) Schematic representation of the adult MB α/β lobe structure and the brain midline, the α/β lobes are shown in magenta, α/β core axons are shown in green.

(B–G) Tet knockdown (KD) using the 201Y-GAL4 MB driver, which also controls the expression of membrane-tethered CD8:GFP. α/β lobes were stained with anti-Fas2 antibody (B, C, magenta), α/β cores were stained with anti-GFP antibody (D, E, green), F and G are merged images of B and D or C and E.

(H) Percentage of β lobe fusion phenotype obtained from RNAi control or Tet KD in (B-G); n = 29–31.

(I) Sequence homology and amino acid conservation of the Tet and CGBP CXXC zinc finger DNA-binding domains.

(J) Sequence homology and amino acid conservation of the human and *Drosophila* Tet 2OGFeDO catalytic domains.

(K–M) MB α/β lobes stained with the anti-Fas2 antibody of Tet domain mutants: DNA-binding domain C to A mutation (Tet^{AXXC}), or catalytic domain HRD to YRA mutation (Tet^{YRA}).

(N) Quantification of (K–M), percentage of normal or β fusion phenotypes, wild-type *WT*, Tet^{AXXC}, and Tet^{YRA}; n = 30–37. Chi-square test with ****$p < 0.0001$, ns $p > 0.05$. Scale bar: 50 μm. See also Figure S1.

domain is mainly responsible for both, the observed phenotype and the regulation of Gs2. The regulation occurs during early brain development and is mediated by the insulin-producing cells (IPCs). Modulating glutamatergic signaling by treating *Tet* mutant with mGluR inhibitor 2-methyl-6-(phenylethynyl)-pyridine (MPEP) or glutamate can respectively rescue or enhance the axon guidance defects in the mutant. Interestingly, *Tet* and *Fmr1* mutants exhibit similar phenotype and Gs2 reduction in the brain, and expressing Gs2 in the IPCs can rescue the phenotype in both mutants, suggesting a functional interaction of the two genes.

RESULTS

Tet controls axon guidance in the brain via its DNA-binding domain

In the *Drosophila* brain, MB lobes are bundles of axons originating from MB neurons. In wild-type brains, axons of these lobes are separated at the brain midline, e.g., the β lobe in the left-brain hemisphere never touches the β lobe on the right side (Figure 1A). To test whether Tet is required for MB axon guidance, we knocked down its expression using RNAi under the control of 201Y-GAL4 driver. This driver is known to express in MB α/β core and γ neurons[28] and in midline cells (this study and see Figure 4A [28]). To assess the effectiveness of Tet RNAi, we examined Tet mRNA levels in larval brains by RT-qPCR using the ubiquitous driver da-GAL4 (Figure S1A). Tet knockdown using

201Y-GAL4 causes MB β axons to cross the midline and fuse with the β axonal bundle from the opposite brain hemisphere causing β lobe fusion (compare Figures 1C–1E, and 1G with Figures 1B–1D, and 1F). 71% of Tet RNAi flies show β lobe fusion while none of the RNAi control flies showed fusion (Figure 1H). Tet RNAi did not affect γ or α lobes (Figures S1B–S1D and Figures 1C–1G). Thus, Tet is required for the guidance of MB β axons. Our previous study found that Tet can regulate robo2 and slit via RNA modification[29]; however, robo2 knockdown using the MB driver 201Y-GAL4 showed only non-significant effects on MB axon outgrowth (Figures S1E–S1H) suggesting that Tet regulates MB axon guidance via different target genes.

Tet has two domains, CXXC zinc finger and 2OGFeDO which are respectively responsible for its DNA-binding or its catalytic activities. The mammalian TET DNA-binding domain can bind to DNA to modulate epigenetic marks or to recruit other epigenetic factors to regulate gene expression.[30–32] The catalytic domain is responsible for converting 5-methylcytosine (5mC) to 5-hydroxymethylcytosine (5hmC) in DNA and RNA.[1,2] To investigate the functions of these domains, we employed a CRISPR/Cas9 and homologous directed repair (HDR) approach to generate targeted point mutations.[33–35] It has previously been shown that mutating one cysteine in the highly conserved zinc finger domain of the CGBP (CpG-binding protein) protein to alanine completely abolishes the ability to bind DNA (Figure 1I).[36] We generated a mutant fly line in which the same conserved cysteine within Tet was substituted by alanine and called the mutation Tet^{AXXC} (Figure 1I). Using the same CRISPR/Cas9 and HDR approach, we also generated a mutant in which the conserved histidine and aspartic acid in the active site of the catalytic domain were substituted by tyrosine and alanine and called the mutation Tet^{YRA} (Figure 1J). This change in amino acids was previously shown to abolish the catalytic function of vertebrate Tet.[1] Both these homozygous mutant fly lines show only partial lethality, unlike homozygous Tet^{null} flies that are completely lethal and die at the late pupal stage (Figures S1I and S1J). We analyzed the changes in MB structure in both mutant lines. By staining the adult brains with anti-Fas2 antibody to visualize the α/β lobes, we found that homozygous Tet^{AXXC} showed the β lobe fusion phenotype in 68%, while, surprisingly, in homozygous Tet^{YRA} the fusion was seen in just 11%, and wild type had 0% β lobe fusion (Figures 1K–1N). Thus, Tet DNA-binding domain is primarily responsible for MB β axon guidance.

Tet is required in early brain development to prevent β axons from crossing the brain midline

MB development starts in early embryogenesis and originates from four neuroblasts (Figure 2A). To determine when during development Tet is required for β axon guidance, we combined the 201Y-GAL4 driver with temperature-sensitive GAL80 ($GAL80^{ts}$) for a temperature shift experiment allowing stage-specific RNAi induction. We selectively induced Tet RNAi from the white prepupal stage (WPP) to adult, WPP to 48 h after puparium formation (APF), or embryo to WPP (Figure 2B). Tet RNAi during embryogenesis and larval development does not cause β axon midline crossing (embryo to WPP), but Tet RNAi during pupation (WPP to adult, WPP to 48h APF) resulted in β fusion observed in the adult brain, similar to what is seen when Tet is depleted throughout development (embryo to adult) (Figure 2C). Tet is therefore specifically required in early pupae for normal β axon guidance. To confirm the temperature shift result, we also dissected and stained Tet^{AXXC} brains with anti-Fas2 antibody at four time points between WPP and 48h APF. We first observed β axons crossing the midline in the Tet^{AXXC} brain 24h APF (Figure 2D). Thus, Tet is required during the first 24h APF to prevent β axons from crossing the brain midline.

Anti-Fas2 staining labels MB axon bundles; however, it cannot reveal how single axons grow. Thus, we employed a stochastic labeling method in which a membrane-tethered molecular marker called smGdP (spaghetti monster Green darkened Protein) was put under the control of the GAL4/UAS and heat shock FLP/FRT inducible systems to generate MultiColor FlpOut (MCFO).[37] This method has been used to label single neurons, axons, and small dendrites at high resolution.[37] To label growing axons, we needed a GAL4 driver that is expressed at that stage. From our temperature shift study above, we knew that Tet itself is active at this stage thus we used Tet-T2A-GAL4, a GAL4 driver expressed under the control of the Tet promoter.[38,39] We expressed smGdP under Tet-T2A-GAL4 control, heat-shocked at the WPP stage, and stained brains at 21 h APF with anti-HA antibody. The result showed that Tet-T2A-GAL4 drove expression in a subset of MB neurons, their axons and importantly, growing axons (Figures S2C–S2F) including β axons projecting their growth cone toward the brain midline. In addition, inducing Tet RNAi by Tet-T2A-GAL4 produced the same β lobe midline crossing phenotype (Figures S2G and S2H) as seen with the 201Y-GAL4 driver (Figures 1B and 1C). Thus, we used the Tet-T2A-GAL4 driver for simultaneously inducing Tet RNAi and labeling growing β axons to see how these axons behave under wild type versus Tet RNAi conditions (see STAR Methods). We found that in Tet RNAi at 21 h APF, some axons at the tip of the left β lobe are protruding and extending their projections over the midline toward the right β lobe (Figures 2H–2J). This phenomenon does not occur in the control (Figures 2E–2G). In this experiment, we look at early prospective adult axon outgrowth. They are likely axons from pioneer α/β neurons[40] involved in the formation of the β lobe observed in the adult brain. In addition to the Tet RNAi axon outgrowth defect, we also noticed that there are small swellings located along the portion of the axon that crossed the midline (Figures 2K and 2L, arrowheads). These swellings are the signs of synaptic boutons indicating that the midline crossing axons, normally restrained to the left-brain hemisphere, likely form synapses with neurons from the right brain hemisphere and potentially affect the MB circuit. Thus, Tet is required to keep β axons confined to one of the two brain hemispheres to prevent any misconnection of β axons between the two sides of the brain.

Tet regulates axon guidance by controlling the levels of glutamine synthetase 2, a key enzyme in glutamatergic signaling

To investigate how Tet controls MB axon guidance at the molecular level, 24 h pupal brains of *wild-type* and Tet^{AXXC} were dissected and subjected to RNA sequencing. The result showed that in the Tet^{AXXC} brains, 1,503 genes are up-regulated and 29 genes down-regulated compared to wild type (Figure 3A, Tables S4 and S5). Most of the up-regulated genes are expressed at low levels and GO term analysis showed that these genes functioned in sperm development and motility (Figures S3A and S3B). But interestingly, the two most significantly down-regulated genes, *Glutamine synthetase 2* (*Gs2*) and *GABA transporter* (*Gat*) (Figure 3A), are the key enzyme of glutamatergic signaling and the key

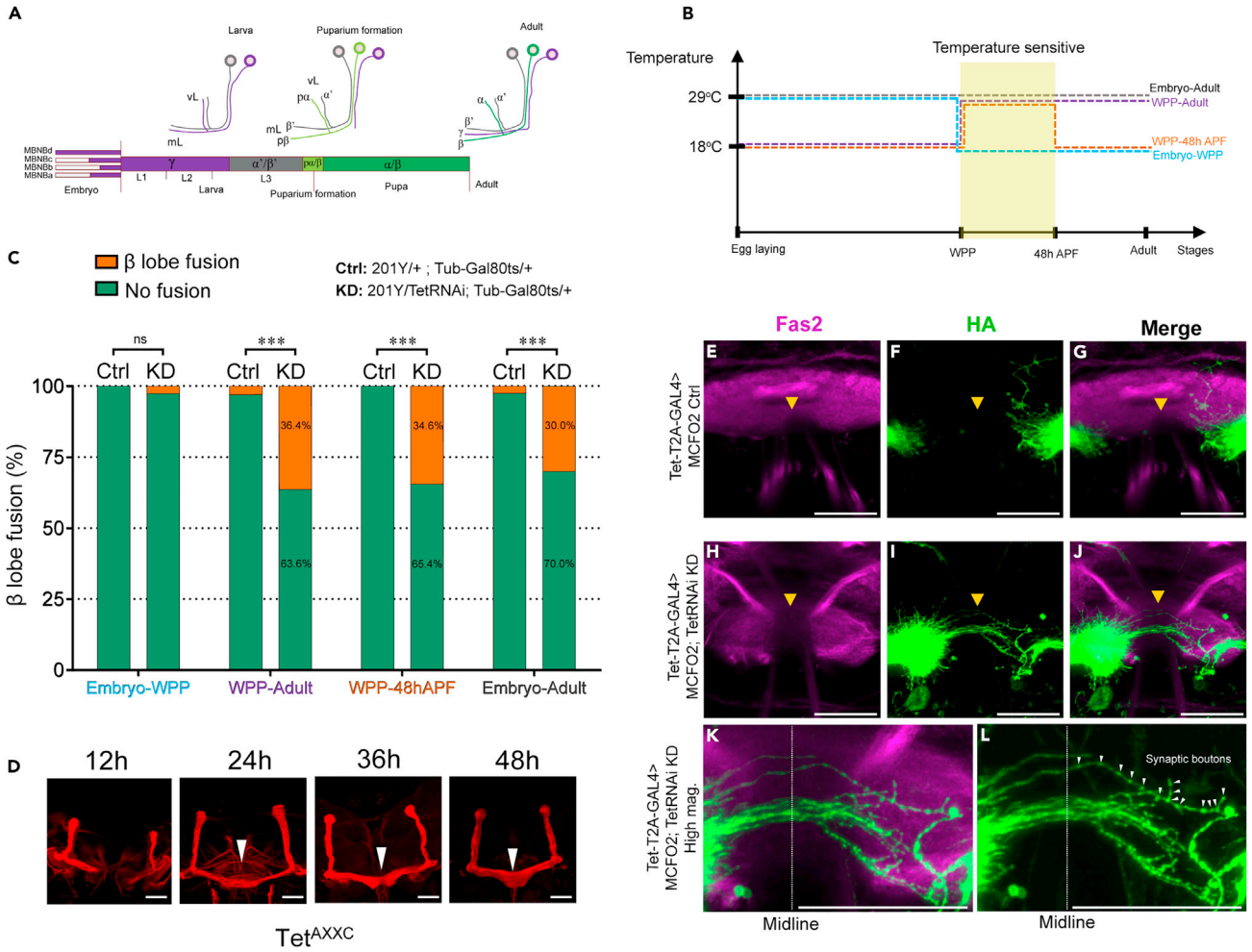

Figure 2. Tet is required in the first 24 h APF to prevent β axons from crossing the brain midline

(A) The progression of MB axon development from four embryonic MB neuroblasts (MBNBs) is depicted (simplified from Kunz et al. 2012 study[16]).

(B) Temperature shift (TS) scheme to knockdown Tet using the GAL4/GAL80^{ts} system at four developmental stages: embryo to adult, WPP to adult, WPP to 48 h APF, embryo to WPP. WPP: white prepupa, APF: after puparium formation.

(C) Percentage of brains with β lobe midline crossing phenotype (orange) in TS Tet KD (201Y > TetRNAi; tub-GAL80^{ts}, KD) and control (201Y> tub-GAL80ts, Ctrl); $n = 29–38$; Chi-square test with $***p < 0.001$, ns $p > 0.05$. Tet KD from embryo to WPP does not affect the growth of β axons, but Tet KD from embryo to adult, WPP to adult, or WPP to 48 h APF resulted in β axon midline crossing. The temperature-sensitive period is indicated in yellow in (B).

(D) *Tet^{AXXC}* pupal brains from different developmental stages (12 h, 24 h, 36 h, and 48 h APF) were stained with anti-Fas2 antibody. β axon midline crossing occurs from 24h APF onward.

(E–L) Stochastic labeling of MB β axons in the developing pupal brain (21 h APF), Tet KD driven by Tet-T2A-GAL4 (H–J, Tet-GAL4> MCFO2, TetRNAi) or control (E–G, Tet-GAL4> MCFO2) brains. Brains were stained with anti-HA antibodies to label axons (green) and anti-Fas2 antibodies (magenta) to label MB and ellipsoid bodies and to locate the brain midline. Tet KD in the developing brain leads to growing axons crossing the midline (I and J), not observed in the control (F and G). (K) and (L) are high magnifications of (J) and (I). Example of an axon in (K) showing the portion of the axon that has crossed the midline with synaptic boutons (L, arrowhead). Scale bars: 25 μm. See also Figure S2.

transporter of GABAergic signaling (Figure 3B). Gs2 can convert glutamate to glutamine and Gat can uptake GABA (Figure 3B),[41–43] suggesting a new and interesting regulation of *Tet* in glutamatergic and GABAergic signaling that potentially affects axon guidance.

To confirm the RNA-sequencing results, we performed RT-qPCR to test the RNA levels of *Gs2* and *Gat* in *wild type* and *Tet^{AXXC}* brains. The result confirmed that both genes are down-regulated in *Tet^{AXXC}* compared to *wild type* (Figure 3C). In addition, because it had been shown that *Fmr1* mutants also exhibit the β lobe fusion phenotype,[21,44] we also dissected 24 h pupal brains of the *Fmr1^{3}* mutant[25] and determined the expression of these same two genes. Interestingly, *Gs2* and *Gat* are also down-regulated in *Fmr1^{3}* (Figure 3C).

Glutamate can control the growth rate of dopaminergic axons[22] and can also reduce the responsiveness of growth cones to repellent cues,[23] and GABA has been shown to control axonal growth.[45,46] Thus, the down-regulation of *Gs2* and *Gat* may be responsible for the MB β axon midline crossing phenotype. To test this hypothesis, we expressed *Gs2* and *Gat* RNAis under the control of the 201Y-GAL4 driver.

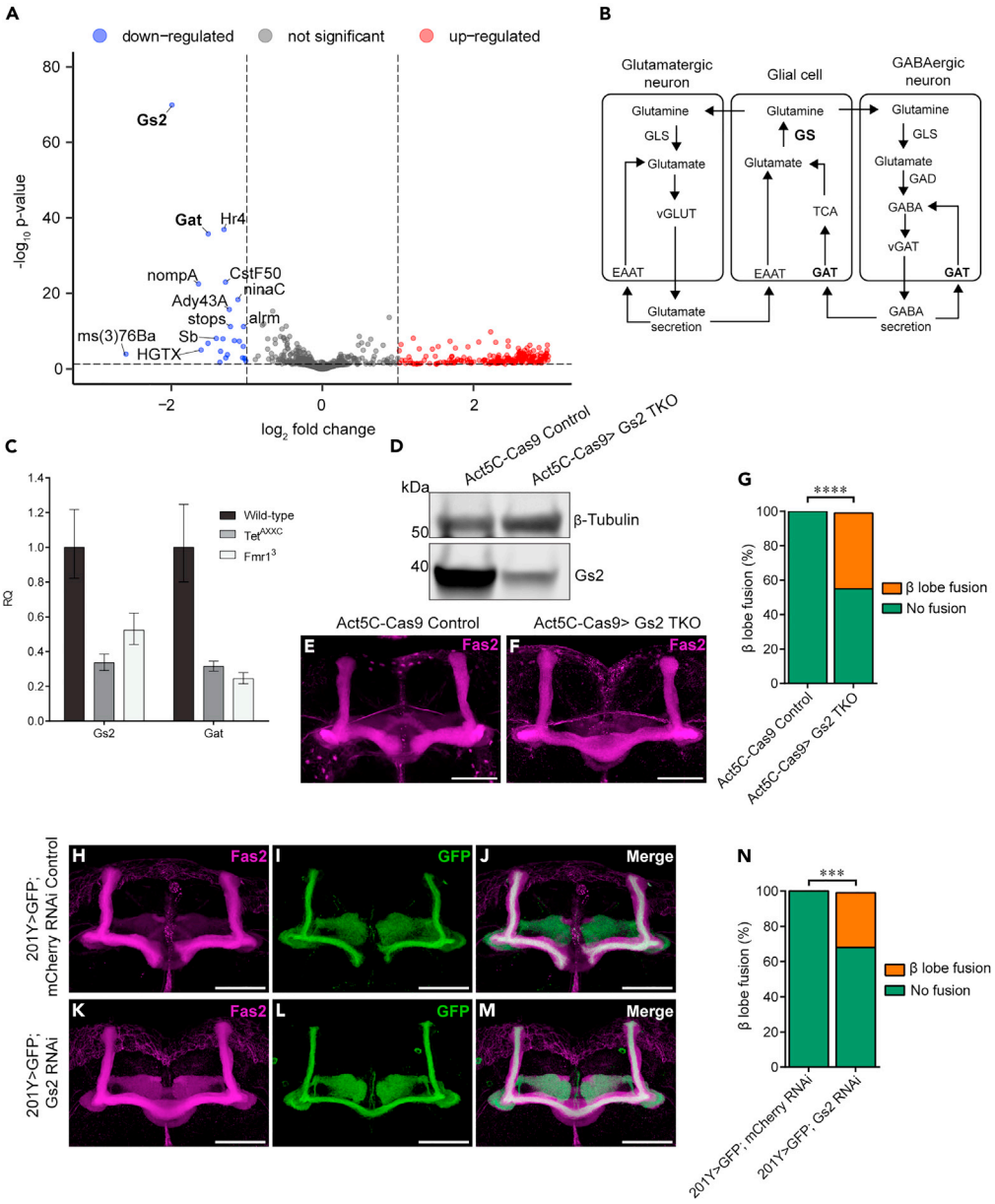

Figure 3. Tet regulates β axon guidance by controlling glutamate synthetase 2 levels in the brain

(A) Volcano plot of RNA sequencing results, showing differentially expressed RNAs in *Tet*^{AXXC} and *wild-type* brains. Significant differences are defined by *p*-value <0.01 and fold change >2.

(B) Representation of the glutamatergic and GABAergic pathways showing that Gs2 and Gat are the main enzyme and transporter, respectively, of the pathway.

(C) Comparison of Gs2 and Gat transcript levels in *wild-type* or *Tet*^{AXXC} and *Fmr1*^{3} mutant brains assessed by RT-qPCR. RQ: relative quantification, error bars represent standard deviation (SD).

(D) Western blot showing Gs2 protein levels in the brains of control (Act5C-Cas9) or CRISPR/Cas9 mutated Gs2 (Act5C-Cas9> Gs2 TKO) blotted with anti-Gs2 antibody.

(E and F) MB α/β lobes stained with anti-Fas2 antibody showing Gs2 mutated brain exhibiting MB β lobe midline crossing (F, Act5C-Cas9> Gs2 TKO) not observed in control brains (E, Act5C-Cas9 Control).

(G) Quantification of phenotype seen in (E andF); *n* = 30–38.

(H–M) Gs2 RNAi KD driven by 201Y-GAL4 (K–M) or control (H–J). All brains express 201Y-GAL4 driven CD8::GFP. Brains were stained with anti-Fas2 and anti-GFP antibodies to visualize whole α/β lobes (Fas2, magenta) or core α/β (GFP, green). Gs2 KD using MB driver 201Y-GAL4 recapitulates the *Tet*^{AXXC} midline crossing phenotype not observed in control.

(N) Quantification of midline crossing phenotype; *n* = 35–39. Chi-square test with ****$p < 0.0001$, ***$p < 0.001$. Scale bars: 50 μm. See also Figures S3 and S4A–S4D, and Table S4 and S5.

Gs2 RNAi produced the β axon midline crossing phenotype similar to what is observed in the Tet^{AXXC} mutant (Figures 3H–3N) suggesting that Tet regulates β axon guidance via Gs2.

When *Gat* RNAi was expressed under the control of 201Y-GAL4 it resulted in early lethality but using a more restricted driver, Dilp2-GAL4, allowed the survival of pupae. Using two different Gat RNAi lines we did not observe any axon defect in the MB, while Tet knockdown with the same driver showed the midline crossing phenotype (Figures S4A–S4D).

To confirm the *Gs2* RNAi phenotype, we inactivated *Gs2* ubiquitously using CRISPR/Cas9-mediated mutagenesi. The mutagenesis was mediated by the combination of ubiquitously expressed Act5C-Cas9 and a Gs2 sgRNA expressing line. The Gs2 mutagenized brains showed a significant reduction of Gs2 protein compared to control brains (Figure 3D). Importantly, 45% of the *Gs2* mutagenized brains showed β axons crossing the midline while no control brains showed this phenotype (Figures 3E–3G). These results validate Tet function in controlling MB β axon guidance by regulating the level of Gs2 in the brain.

Tet acts in insulin-producing cells (IPCs) to regulate axon guidance

Expressing *Tet* or *Gs2* RNAi under the control of the mushroom body 201Y-GAL4 driver results in the β lobe midline crossing phenotype. However, exactly which cells in the brain express Gs2 to control MB organization is not known. At 24 h APF, 201Y-GAL4 expresses in both MB neurons and a group of cells at the midline of the brain named midline cells (MLCs) (Figure 4A). To examine if the MB neurons and/or MLCs express Gs2, brains were stained with anti-Gs2 antibody.[47] In brains expressing CD8::GFP driven by 201Y-GAL4, the Gs2 antibody (magenta) does not stain the MB neurons (Figures 4B–4D) but strongly stains the MLCs (Figures 4E–4G, asterisks). Another MB driver, OK107-GAL4, also expresses in these MLCs, mostly commonly called insulin-producing cells (IPCs).[48] In addition, Cao et al., have shown that Gs2 is highly enriched in IPCs.[49] Thus, we suspect that the MLCs that express 201Y-GAL4 are IPCs, and concluded that Tet may regulate Gs2 in IPCs. To test this hypothesis, we drove *Tet* or *Gs2* RNAis using a Dilp2-GAL4 driver, which is expressed specifically in IPCs. Knocking down Tet or Gs2 in the IPCs produced an MB β axon crossing phenotype similar to that observed in Tet^{AXXC} (Figures 4H–4K). We found that Tet is also expressed in the IPCs by expressing Tet-T2A-GAL4 driver and co-stained with anti-Dilp2 antibody (Figures S2I–S2L) confirming the requirement of Tet and Gs2 in the IPCs for regulating MB axon guidance.

Tet and *Fmr1* mutant phenotypes can be rescued by expressing Gs2 in IPCs

To validate that Tet and Gs2 act in IPCs to regulate β axon guidance we tested if the Tet^{AXXC} phenotype could be rescued by expressing a Gs2 transgene in IPCs specifically. For these rescue experiments Tet^{AXXC} mutants that expressed Gs2 in the IPCs (*Dilp2-GAL4/UAS-Gs2*; Tet^{AXXC}/Tet^{AXXC}) (Figure 4N) were compared to the mutant control, Tet^{AXXC} mutants that did not express Gs2 (*Dilp2-GAL4/+*; Tet^{AXXC}/Tet^{AXXC}) (Figure 4M) and the wild-type control (*Dilp2-GAL4/+*) (Figure 4L). Results showed that while Dilp2-GAL4 alone did not affect the β axon guidance, expressing Gs2 in the IPCs of Tet^{AXXC} brains can significantly reduce the Tet^{AXXC} phenotype (26% MB fusion) compared to Tet^{AXXC} flies without Gs2 expression (47% MB fusion, Figure 4O).

Since *Tet* and *Fmr1* mutants exhibit similar phenotypes and downregulation of Gs2, the same experimental design was applied to rescue $Fmr1^{3}$ mutants (Figures 4L–4N). When Gs2 is expressed in the IPCs of the $Fmr1^{3}$ mutant brains, the structural defect was also reduced (21% MB fusion) compared to the homozygous mutant $Fmr1^{3}$ brains (54% MB fusion, Figure 4P). Taken together, these results demonstrate that Tet and Gs2 act in the IPCs to regulate MB β axon guidance. The results also suggest an important interaction of Tet and Fmr1 in regulating axon guidance via Gs2.

Axon guidance defects in *Tet* mutants are modulated by glutamatergic signaling

Gs2 is a key enzyme in glutamatergic signaling. Our results showed that Gs2 is regulated by Tet to control β axon guidance. In *Tet* mutant brains, the reduction of Gs2 may lead to the accumulation of glutamate and upregulation of glutamatergic signaling. Excess amounts of glutamatergic signaling have been proposed as the main cause of FXS.[50] In fact, treating *Fmr1* mutants with metabotropic glutamate receptor (mGluR) antagonist MPEP can suppress the *Fmr1* mutant phenotypes[21] while treating the mutants with glutamate can enhance the phenotypes.[51] To validate the function of Tet in modulating glutamatergic signaling, we examined if mGluR antagonist MPEP and glutamate can affect the *Tet* mutant phenotype. *Wild-type* and Tet^{AXXC} third-instar larvae were transferred to food suppl

emented with MPEP or glutamate as treatments, or water as control (Figure 4Q). The treatment had no negative effect on viability (Figure S4E). Brains from 5- to 10-day-old flies were dissected and stained with anti-Fas2 antibody and the percentage of brains showing MB β midline crossing was quantified. The result showed that treating Tet^{AXXC} mutants with glutamate increased the number of flies with the β axon crossing midline phenotype by 27% while treating with MPEP showed 17% reduction of the phenotype compared to the non-treated control (Figure 4R). Neither of the treatments affected *wild-type* brains (Figure 4R). Thus, modulating glutamatergic signaling by glutamate or the mGluR antagonist MPEP can enhance or suppress respectively the β axon guidance defects in Tet^{AXXC} mutant. This result confirms the function of Tet in regulating glutamatergic signaling to control axon guidance in the brain.

DISCUSSION

Tet controls axon guidance during early brain development via its DNA-binding domain

TET is essential for neurodevelopment,[52] but how it functions Tet in the developing brain is not well understood. For instance, TET3 is upregulated and required for axon regeneration in adult dorsal root ganglion (DRG) neurons after injury,[53] and Tet is involved in neuronal functions

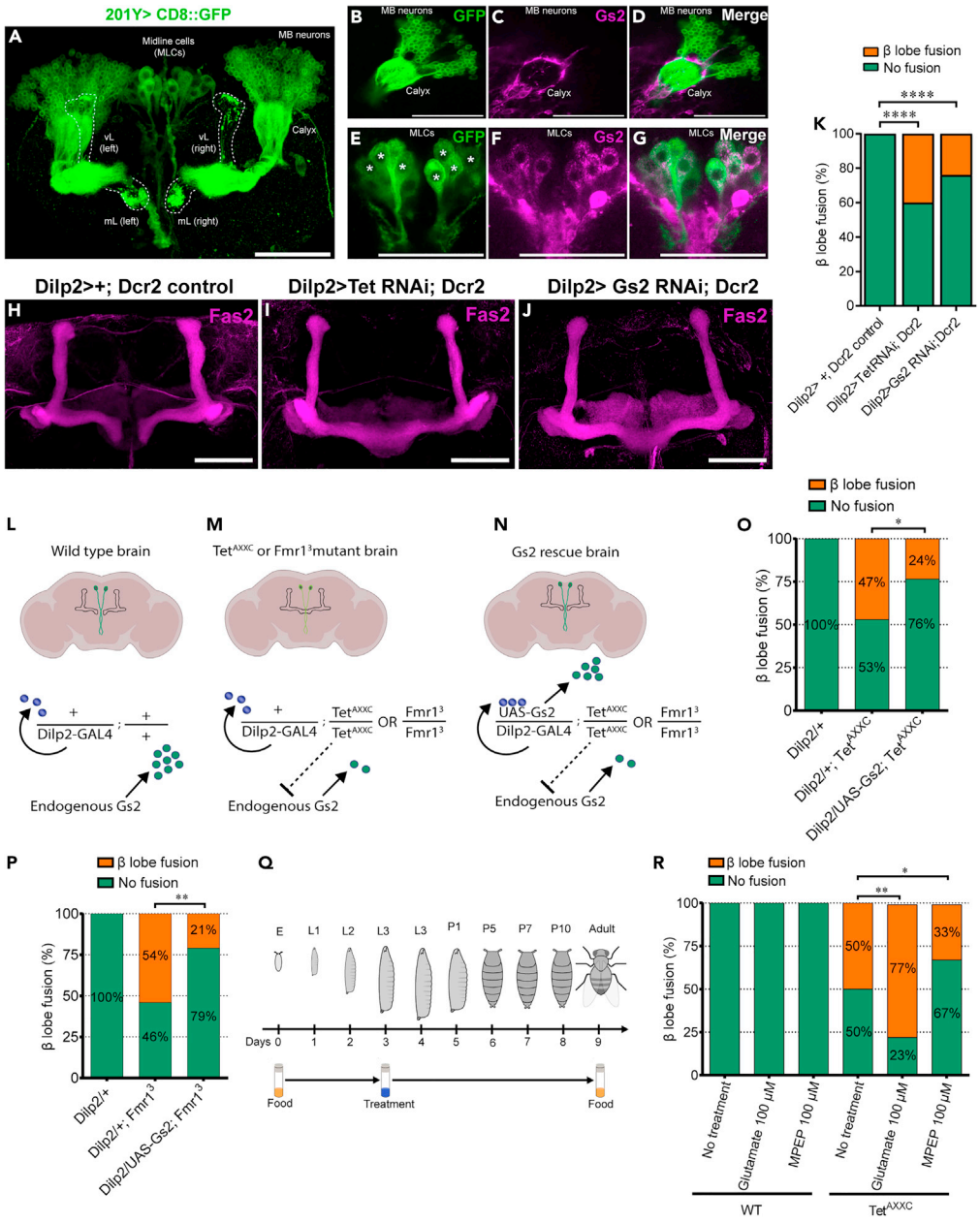

Figure 4. Tet regulates β axon guidance via insulin-producing cells (IPCs) and the *Tet* and *Fmr1* mutant phenotypes can be rescued by overexpressing Gs2 in the IPCs or by MPEP treatment

(A) 201Y-GAL4 driven membrane-tagged CD8::GFP expression pattern in 24 h APF brain, the driver expresses in MB neurons and midline cells (MLCs). vL: vertical lobe, mL: medial lobe.

(B–G) 201Y-GAL4 driven CD8::GFP cells (green) and Gs2 expressing cells (magenta, anti-Gs2 staining). Gs2 is not expressed in MB neurons (B–D) but instead is expressed in MLCs (E–G, asterisks marks midline cells expressing Gs2).

(H–J) MB α/β lobes stained with anti-Fas2 antibody in the Dilp2-GAL4 driver control (H), Dilp2-GAL4 driven Tet RNAi (I), or Dilp2-GAL4 driven Gs2 RNAi (J). (K) Quantification of β fusion brain in (H–J); n = 41–45.

(L—N) Schematic representation of the experimental design for rescuing *Tet* or *Fmr1* mutant phenotypes by expressing Gs2 under the control of Dilp2-GAL4.

(O) Percentage of brains showing MB β axon midline crossing from wild type, *Tet*^{AXXC} mutants, and Gs2 rescued *Tet*^{AXXC} mutants; n = 37–49.

(P) Percentage of brains from wild type, *Fmr1*^{3} mutants, and Gs2 rescued *Fmr1*^{3} mutants showing MB β axon midline crossing; n = 30–33.

(Q) MPEP and glutamate treatment scheme for *wild-type* and *Tet*^{AXXC} mutant flies. Third-instar larvae were reared on food containing MPEP or glutamate and changed to normal food after eclosion.

(R) Percentage of *wild type* or *Tet*^{AXXC} mutant brains showing MB β axon midline crossing after MPEP or glutamate treatment; n = 31–48. Chi-square test with $*p < 0.05$, $**p < 0.01$, $****p < 0.0001$. Scale bar: 50 μm. See also Figures S2I–S2L, and S4E.

including commissure axon patterning and glial homeostasis in *Drosophila*.[4,54,55] However, the requirement of Tet and its DNA-binding domain in regulating axon guidance in the developing brain has not been studied. Our results establish that Tet regulates the guidance of β axons in the MB, a prominent structure in the brain that controls different neurological functions,[14,15] and this regulation is dependent on its DNA-binding domain.

Our results also show that the requirement for Tet function in the MB β axon guidance is limited to the first 48 h of pupal brain development, at a time when β axons grow to form the mature MB β lobes. When Tet levels are reduced β axons are not restricted to one hemisphere, rather they grow across the brain midline. Careful inspection of the Tet RNAi axons that cross the midline showed that these axons formed synaptic boutons in the "wrong" brain hemisphere suggesting that the circuits of the hemispheres are misconnected. Together these observations suggest that treatment for neurodevelopmental disorders that are due to axon guidance problems and the ensuing misconnection of synapses needs to be applied at early stages of nervous system development.

Tet regulates glutamatergic signaling

Our transcriptomic studies demonstrated that *Gs2* and *Gat* are generally regulated by *Tet* in the brain, but here we concentrated on their requirement in the MB. Gs2 is a key enzyme in regulating glutamate levels in glutamatergic signaling and Gat is the neurotransporter that controls GABA levels in the GABAergic signaling suggesting that Tet is required in both pathways. However, knockdown of Gat did not result in an β lobe phenotype suggesting that Gat is not required for normal axon guidance. In contrast, inducing Gs2 RNAi by the 201Y-GAL4 driver resulted in axon defects suggesting that MB axon guidance is regulated by glutamatergic signaling via Gs2. In addition, treating Tet^{AXXC} mutants with MPEP, a metabotropic glutamate receptor (mGluR) antagonist,[21] can partially rescue the axon guidance defects while feeding mutants glutamate enhances the Tet^{AXXC} phenotype. These data demonstrate a new function of Tet in regulating glutamatergic signaling in the brain and support the notion that the pathway is mis-regulated in Tet mutant brains. Glutamatergic signaling is a major excitatory signal in the human brain and the pathway is also known to act in neural developmental events such as proliferation, differentiation, migration, and synaptogenesis.[19] Interestingly, elevated levels of glutamatergic signaling have also been proposed as the underlying mechanism of the neurodevelopmental disorder in FXS.[50] Based on the conserved functional domains of Tet in humans and flies, the mis-regulation of the glutamatergic signaling we observed in *Drosophila* brain during early development may also occur in developing human brains harboring Tet mutations that lead to neurodevelopmental disorders.

We have previously mapped Tet-DNA -binding sites in the genome by ChIP-seq and mapped Tet-mediated 5hmrC RNA modification throughout the transcriptome by hMeRIP-seq.[29] There is no Tet binding detected by ChIP-seq on the gene body or promoter region of *Gs2* and *Gat* (Figures S3C–S3E). In addition, the Gs2 and Gat mRNAs do not carry the Tet-dependent 5hmrC modification.[29] These observations suggest that Tet regulates *Gs2* and *Gat* indirectly. We investigated if robo2/slit, which we identified as RNA modification targets of Tet, could regulate MB axon guidance. However, we observed no significant effects on MB axon guidance upon robo2 knockdown in the MB. Therefore, we propose that one or several Tet target genes are responsible for controlling the transcription or RNA levels of Gs2 and Gat.

Alternatively, Tet may have a novel, so far unknown function. Since *Gs2* and *Gat* are also down-regulated in the $Fmr1^{3}$ mutant, *Tet* and *Fmr1* may function together to control the mRNA levels of these two and potentially additional genes. Fmr1 was previously found in the regulatory protein complex Not1/CCR4,[56] which is known to control all steps of gene expression from transcription in the nucleus to mRNA degradation in the cytoplasm depending on the composition of proteins that interact with the complex.[57] In this case the DNA-binding domain of Tet may be responsible for protein-protein interaction(s) necessary to form the complex. We have previously identified Fmr1 in a complex with the zinc finger protein RP-8 (Zfrp8), which functions in the assembly of mRNA ribonucleoprotein (mRNP) complexes.[58] Interestingly, by co-immunoprecipitation we found Zfrp8 and Tet in the same complex (Figure S3F). Thus, Tet and Fmr1 may both coordinate with the Not1/CCR4 or other mRNP complexes to regulate the expression levels of *Gs2* and *Gat*. Indeed, understanding these complexes and their functions in controlling mRNA levels is of great importance, especially since RNA processing is not well understood.

Tet and Gs2 are required in the insulin-producing cells (IPCs) to regulate axon guidance

IPCs in *Drosophila* are a group of neurons located at the dorsal midline of the central brain that produce and secrete insulin-like peptides into the hemolymph to regulate growth and metabolism.[59,60] Previous studies have shown that IPCs can also regulate neuronal functions.[61,62] For instance, overexpressing Fmr1 in IPCs could rescue the circadian defects observed in *Fmr1* mutants.[63] But the involvement of IPCs in regulating MB axon guidance has not previously been shown. In our RNA-seq experiments, *Gs2* is the most significantly reduced transcript in the Tet^{AXXC} mutant brain. We found that Gs2 is expressed in the IPCs but not in MB neurons. We observed that Tet is also expressed in IPCs and in agreement with this expression we detect the axon midline-crossing phenotype when we specifically knock down either Tet or Gs2 in IPCs. In addition, the axon midline-crossing phenotype was rescued when expressing Gs2 in the IPCs of *Tet* and *Fmr1* mutants. Hence, our results point to a previously unknown function of IPCs in regulating MB axon guidance via glutamatergic signaling in the developing brain.

In addition to IPCs,[49] Gs2 is also expressed in glial cells where it is responsible for converting glutamate to glutamine to regulate the levels of the neurotransmitter glutamate in the brain.[64,65] Thus, the reduction of Gs2 levels in Tet^{AXXC} mutants may lead to the accumulation of glutamate and a deficiency of glutamine in the IPCs. However, the mechanism by which Tet and Gs2 regulate axon guidance via IPCs needs to be further elucidated. One possible mechanism is that in Tet mutant brains Gs2 is reduced in the IPCs leading to the accumulation of glutamate in the IPCs that is then secreted at the brain midline. The elevated levels of glutamate at the midline could cause MB β axons to cross over the midline. In support of this possible mechanism, glutamate has been reported to reduce the responsiveness of axonal growth cones to repellent cues such as Slit-2 and Sema-3A/C[23] and also to enhance the growth rate and branching of dopaminergic axons.[22] In addition, glutamate

can be released by pancreatic cells, which are the insulin-secreting cells in mammals, via excitatory amino acid transporters (EAAT) by uptake reversal.[66] The uptake reversal activity of EAAT has also been reported in astrocytes and it depends on the relative intracellular and extracellular glutamate concentration.[67] Further studies are needed to test the secretion of glutamate by IPCs and to investigate whether the MB β axon crossing phenotype is due to elevated glutamate levels at the midline of Tet^{AXXC} mutant brains.

Potential interplay between Tet and Fmr1

Previously, the glutamate receptor antagonist MPEP was successfully used to suppress the axonal defect in $Fmr1^3$ mutants[21] while high glutamate concentration can enhance the phenotype.[51] Our observation that MPEP and glutamate have similar effects on the Tet^{AXXC} phenotype suggests that Tet and Fmr1 have overlapping functions. This conclusion is further strengthened by our finding that Gs2 is down-regulated in the brain of both Tet^{AXXC} and $Fmr1^3$ mutants and that increasing Gs2 levels by overexpressing it from a transgene reduced the occurrence of the β lobe fusion phenotype in both Tet^{AXXC} and $Fmr1^3$ mutants (Figures 4L–4P). The rescue is partial, suggesting that the expression levels of Gs2 are essential additional targets of Tet and Fmr1 may also contribute to the phenotype. As Tet and Fmr1 can regulate a broad spectrum of genes, it is impressive that overexpression of only one gene, Gs2, encoding a key enzyme in the glutamatergic pathway, can rescue the axonal defect in about half of both *Tet* and *Fmr1* mutants.

Dysfunction of glutamatergic signaling is involved in a variety of human diseases including FXS, autism spectrum disorder, schizophrenia, neurodegenerative diseases, and gliomas.[50,68–70] Our results suggest that glutamine synthetase is a potential target for early intervention. Recently, an increasing number of studies have shown that Tet mutations are associated with neurodevelopmental disorders in humans.[8–11] The mechanism by which human TET mutations cause these disorders needs to be elucidated, but the highly conserved functional domains of human and *Drosophila* Tet suggest that the Tet function in axon guidance that we found in *Drosophila* may be conserved in humans. Thus, our study provides initial evidence that glutamatergic signaling is altered in the Tet mutant brains and the mutant may serve as a *Drosophila* model for drug screening and study of neurodevelopmental disorders caused by TET mutations.

Limitations of the study

In this study, we described the new function of Tet in controlling axon guidance in the *Drosophila* brain by regulating glutamatergic signaling via Gs2. We show that Tet indirectly regulates Gs2 levels and suggest a possible underlying mechanism. However further studies need to be conducted to confirm how Tet regulates Gs2 transcript levels. We also demonstrate that Tet and Gs2 are required in the IPCs to control axon guidance. How glutamate is secreted from IPCs and becomes localized to the brain midline and how the outgrowth of the MB axons is misguided by excess glutamate is not known. Identifying a transporter (e.g., EAAT) in the IPCs that is responsible for the secretion of glutamate and a receptor on the MB axons that is responsible for the guidance is necessary to understand the mechanism of how the IPCs regulate MB axons via the neurotransmitter glutamate.

STAR★METHODS

Detailed methods are provided in the online version of this paper and include the following:

- KEY RESOURCES TABLE
- RESOURCE AVAILABILITY
  - Lead contact
  - Materials availability
  - Data and code availability
- EXPERIMENTAL MODELS AND STUDY PARTICIPANT DETAILS
  - Fly stocks
- METHOD DETAILS
  - Generating targeted Tet^{AXXC} and Tet^{YRA} mutants using CRISPR/Cas9 and HDR
  - Lethality
  - Conditional knockdown using temperature shift $GAL80^{ts}$
  - Simultaneously knockdown and visualizing growing axons using Tet-T2A-GAL4
  - Brain dissection, immunostaining and imaging
  - Total RNA isolation
  - Quantitative reverse transcription PCR (RT-qPCR)
  - RNA-seq library generation
  - RNA-seq data analysis
  - Western blot
  - MPEP and glutamate treatment
  - Generating UAS-Gs2 transgene stocks
- QUANTIFICATION AND STATISTICAL ANALYSIS

SUPPLEMENTAL INFORMATION

Supplemental information can be found online at https://doi.org/10.1016/j.isci.2024.109634.

ACKNOWLEDGMENTS

We thank Kenneth Irvine, Cordelia Rauskolb, and Nicholas Stavropoulos for helpful comments on the manuscript. We want to thank Fei Wang, Kishan Bulsara, Anna Zhang, and Ethan Chiang for preliminary data and the Irvine, Barber, and Stavropoulos laboratories for helpful discussion and technical support. We thank Thomas A. Jongens and Eric Rulifson for fly stocks and Pierre Leopold for the Dilp2 antibody. We also thank Svetlana Minakhina for the co-IP result in Figure S3F. We acknowledge the *Drosophila* Genomics Resource Center, Bloomington *Drosophila* Stock Center, Vienna *Drosophila* Resource Center and Developmental Studies Hybridoma Bank for cDNA, fly stocks, and antibodies. This work was supported by grants from the National Institute of General Medical Sciences grant, (5R01GM120405) to R.S., the Vietnam Education Foundation (VEF), and Charles and Johanna Busch pre-doctoral fellowships to H.T.

AUTHOR CONTRIBUTIONS

Conceptualization, H.T. and R.S.; data curation, H.T., L.L., B.N.S., J.K., and R.S.; formal analysis, H.T. and R.S.; funding acquisition, R.S.; investigation, H.T., L.L., B.N.S., and J.K.; methodology, H.T., L.L., B.N.S., J.K., and R.S.; project administration, H.T. and R.S.; resources, H.T., L.L., B.N.S., J.K., and R.S.; software, H.T.; supervision, R.S.; validation, H.T., L.L., J.K., and R.S.; visualization, H.T.; writing – original draft, H.T.; writing – review and editing, H.T., J.K., and R.S.

DECLARATION OF INTERESTS

The authors declare no competing interests.

Received: August 14, 2023
Revised: December 18, 2023
Accepted: March 26, 2024
Published: April 1, 2024

REFERENCES

1. Tahiliani, M., Koh, K.P., Shen, Y., Pastor, W.A., Bandukwala, H., Brudno, Y., Agarwal, S., Iyer, L.M., Liu, D.R., Aravind, L., and Rao, A. (2009). Conversion of 5-methylcytosine to 5-hydroxymethylcytosine in mammalian DNA by MLL partner TET1. Science *324*, 930–935. https://doi.org/10.1126/science.1170116.
2. Fu, L., Guerrero, C.R., Zhong, N., Amato, N.J., Liu, Y., Liu, S., Cai, Q., Ji, D., Jin, S.G., Niedernhofer, L.J., et al. (2014). Tet-mediated formation of 5-hydroxymethylcytosine in RNA. J. Am. Chem. Soc. *136*, 11582–11585. https://doi.org/10.1021/ja505305z.
3. Delatte, B., Wang, F., Ngoc, L.V., Collignon, E., Bonvin, E., Deplus, R., Calonne, E., Hassabi, B., Putmans, P., Awe, S., et al. (2016). RNA biochemistry. Transcriptome-wide distribution and function of RNA hydroxymethylcytosine. Science *351*, 282–285. https://doi.org/10.1126/science.aac5253.
4. Yao, B., Li, Y., Wang, Z., Chen, L., Poidevin, M., Zhang, C., Lin, L., Wang, F., Bao, H., Jiao, B., et al. (2018). Active N(6)-Methyladenine Demethylation by DMAD Regulates Gene Expression by Coordinating with Polycomb Protein in Neurons. Mol. Cell *71*, 848–857.e6. https://doi.org/10.1016/j.molcel.2018.07.005.
5. Dai, H.Q., Wang, B.A., Yang, L., Chen, J.J., Zhu, G.C., Sun, M.L., Ge, H., Wang, R., Chapman, D.L., Tang, F., et al. (2016). TET-mediated DNA demethylation controls gastrulation by regulating Lefty-Nodal signalling. Nature *538*, 528–532. https://doi.org/10.1038/nature20095.
6. Wang, F., Minakhina, S., Tran, H., Changela, N., Kramer, J., and Steward, R. (2018). Tet protein function during Drosophila development. PLoS One *13*, e0190367. https://doi.org/10.1371/journal.pone.0190367.
7. Melamed, P., Yosefzon, Y., David, C., Tsukerman, A., and Pnueli, L. (2018). Tet Enzymes, Variants, and Differential Effects on Function. Front. Cell Dev. Biol. *6*, 22. https://doi.org/10.3389/fcell.2018.00022.
8. Beck, D.B., Petracovici, A., He, C., Moore, H.W., Louie, R.J., Ansar, M., Douzgou, S., Sithambaram, S., Cottrell, T., Santos-Cortez, R.L.P., et al. (2020). Delineation of a Human Mendelian Disorder of the DNA Demethylation Machinery: TET3 Deficiency. Am. J. Hum. Genet. *106*, 234–245. https://doi.org/10.1016/j.ajhg.2019.12.007.
9. Seyama, R., Tsuchida, N., Okada, Y., Sakata, S., Hamada, K., Azuma, Y., Hamanaka, K., Fujita, A., Koshimizu, E., Miyatake, S., et al. (2022). Two families with TET3-related disorder showing neurodevelopmental delay with craniofacial dysmorphisms. J. Hum. Genet. *67*, 157–164. https://doi.org/10.1038/s10038-021-00986-y.
10. Santos-Cortez, R.L.P., Khan, V., Khan, F.S., Mughal, Z.U.N., Chakchouk, I., Lee, K., Rasheed, M., Hamza, R., Acharya, A., Ullah, E., et al. (2018). Novel candidate genes and variants underlying autosomal recessive neurodevelopmental disorders with intellectual disability. Hum. Genet. *137*, 735–752. https://doi.org/10.1007/s00439-018-1928-6.
11. Harripaul, R., Vasli, N., Mikhailov, A., Rafiq, M.A., Mittal, K., Windpassinger, C., Sheikh, T.I., Noor, A., Mahmood, H., Downey, S., et al. (2018). Mapping autosomal recessive intellectual disability: combined microarray and exome sequencing identifies 26 novel candidate genes in 192 consanguineous families. Mol. Psychiatry *23*, 973–984. https://doi.org/10.1038/mp.2017.60.
12. Engle, E.C. (2010). Human genetic disorders of axon guidance. Cold Spring Harb. Perspect. Biol. *2*, a001784. https://doi.org/10.1101/cshperspect.a001784.
13. Strausfeld, N.J., Hansen, L., Li, Y., Gomez, R.S., and Ito, K. (1998). Evolution, discovery, and interpretations of arthropod mushroom bodies. Learn. Mem. *5*, 11–37.
14. Aso, Y., Sitaraman, D., Ichinose, T., Kaun, K.R., Vogt, K., Belliart-Guérin, G., Plaçais, P.Y., Robie, A.A., Yamagata, N., Schnaitmann, C., et al. (2014). Mushroom body output neurons encode valence and guide memory-based action selection in Drosophila. Elife *3*, e04580. https://doi.org/10.7554/eLife.04580.
15. Li, Q., Jang, H., Lim, K.Y., Lessing, A., and Stavropoulos, N. (2021). insomniac links the development and function of a sleep-regulatory circuit. Elife *10*, e65437. https://doi.org/10.7554/eLife.65437.
16. Kunz, T., Kraft, K.F., Technau, G.M., and Urbach, R. (2012). Origin of Drosophila mushroom body neuroblasts and generation of divergent embryonic lineages. Development *139*, 2510–2522. https://doi.org/10.1242/dev.077883.
17. Riedel, G., Platt, B., and Micheau, J. (2003). Glutamate receptor function in learning and memory. Behav. Brain Res. *140*, 1–47. https://doi.org/10.1016/s0166-4328(02)00272-3.
18. Mattson, M.P. (2008). Glutamate and neurotrophic factors in neuronal plasticity and disease. Ann. N. Y. Acad. Sci. *1144*,

97–112. https://doi.org/10.1196/annals.1418.005.
19. Luján, R., Shigemoto, R., and López-Bendito, G. (2005). Glutamate and GABA receptor signalling in the developing brain. Neuroscience *130*, 567–580. https://doi.org/10.1016/j.neuroscience.2004.09.042.
20. Wang, P.Y., Petralia, R.S., Wang, Y.X., Wenthold, R.J., and Brenowitz, S.D. (2011). Functional NMDA receptors at axonal growth cones of young hippocampal neurons. J. Neurosci. *31*, 9289–9297. https://doi.org/10.1523/jneurosci.5639-10.2011.
21. McBride, S.M.J., Choi, C.H., Wang, Y., Liebelt, D., Braunstein, E., Ferreiro, D., Sehgal, A., Siwicki, K.K., Dockendorff, T.C., Nguyen, H.T., et al. (2005). Pharmacological rescue of synaptic plasticity, courtship behavior, and mushroom body defects in a Drosophila model of fragile X syndrome. Neuron *45*, 753–764. https://doi.org/10.1016/j.neuron.2005.01.038.
22. Schmitz, Y., Luccarelli, J., Kim, M., Wang, M., and Sulzer, D. (2009). Glutamate controls growth rate and branching of dopaminergic axons. J. Neurosci. *29*, 11973–11981. https://doi.org/10.1523/jneurosci.2927-09.2009.
23. Kreibich, T.A., Chalasani, S.H., and Raper, J.A. (2004). The neurotransmitter glutamate reduces axonal responsiveness to multiple repellents through the activation of metabotropic glutamate receptor 1. J. Neurosci. *24*, 7085–7095. https://doi.org/10.1523/JNEUROSCI.0349-04.2004.
24. Santoro, M.R., Bray, S.M., and Warren, S.T. (2012). Molecular mechanisms of fragile X syndrome: a twenty-year perspective. Annu. Rev. Pathol. *7*, 219–245. https://doi.org/10.1146/annurev-pathol-011811-132457.
25. Dockendorff, T.C., Su, H.S., McBride, S.M.J., Yang, Z., Choi, C.H., Siwicki, K.K., Sehgal, A., and Jongens, T.A. (2002). Drosophila lacking dfmr1 activity show defects in circadian output and fail to maintain courtship interest. Neuron *34*, 973–984. https://doi.org/10.1016/s0896-6273(02)00724-9.
26. Zhang, Y.Q., Bailey, A.M., Matthies, H.J., Renden, R.B., Smith, M.A., Speese, S.D., Rubin, G.M., and Broadie, K. (2001). Drosophila fragile X-related gene regulates the MAP1B homolog Futsch to control synaptic structure and function. Cell *107*, 591–603. https://doi.org/10.1016/s0092-8674(01)00589-x.
27. Bolduc, F.V., Bell, K., Cox, H., Broadie, K.S., and Tully, T. (2008). Excess protein synthesis in Drosophila fragile X mutants impairs long-term memory. Nat. Neurosci. *11*, 1143–1145. https://doi.org/10.1038/nn.2175.
28. Redt-Clouet, C., Trannoy, S., Boulanger, A., Tokmatcheva, E., Savvateeva-Popova, E., Parmentier, M.L., Preat, T., and Dura, J.M. (2012). Mushroom body neuronal remodelling is necessary for short-term but not for long-term courtship memory in Drosophila. Eur. J. Neurosci. *35*, 1684–1691. https://doi.org/10.1111/j.1460-9568.2012.08103.x.
29. Singh, B.N., Tran, H., Kramer, J., Kirichenko, E., Changela, N., Wang, F., Feng, Y., Kumar, D., Tu, M., Lan, J., et al. (2024). Tet-dependent 5-hydroxymethyl-Cytosine modification of mRNA regulates axon guidance genes in Drosophila. PLoS One *19*, e0293894. https://doi.org/10.1371/journal.pone.0293894.
30. Rasmussen, K.D., and Helin, K. (2016). Role of TET enzymes in DNA methylation, development, and cancer. Genes Dev. *30*, 733–750. https://doi.org/10.1101/gad.276568.115.
31. Williams, K., Christensen, J., Pedersen, M.T., Johansen, J.V., Cloos, P.A.C., Rappsilber, J., and Helin, K. (2011). TET1 and hydroxymethylcytosine in transcription and DNA methylation fidelity. Nature *473*, 343–348. https://doi.org/10.1038/nature10066.
32. Deplus, R., Delatte, B., Schwinn, M.K., Defrance, M., Méndez, J., Murphy, N., Dawson, M.A., Volkmar, M., Putmans, P., Calonne, E., et al. (2013). TET2 and TET3 regulate GlcNAcylation and H3K4 methylation through OGT and SET1/COMPASS. EMBO J. *32*, 645–655. https://doi.org/10.1038/emboj.2012.357.
33. Gratz, S.J., Wildonger, J., Harrison, M.M., and O'Connor-Giles, K.M. (2013). CRISPR/Cas9-mediated genome engineering and the promise of designer flies on demand. Fly (Austin) *7*, 249–255. https://doi.org/10.4161/fly.26566.
34. Gratz, S.J., Ukken, F.P., Rubinstein, C.D., Thiede, G., Donohue, L.K., Cummings, A.M., and O'Connor-Giles, K.M. (2014). Highly specific and efficient CRISPR/Cas9-catalyzed homology-directed repair in Drosophila. Genetics *196*, 961–971. https://doi.org/10.1534/genetics.113.160713.
35. Gratz, S.J., Cummings, A.M., Nguyen, J.N., Hamm, D.C., Donohue, L.K., Harrison, M.M., Wildonger, J., and O'Connor-Giles, K.M. (2013). Genome engineering of Drosophila with the CRISPR RNA-guided Cas9 nuclease. Genetics *194*, 1029–1035. https://doi.org/10.1534/genetics.113.152710.
36. Lee, J.H., Voo, K.S., and Skalnik, D.G. (2001). Identification and characterization of the DNA binding domain of CpG-binding protein. J. Biol. Chem. *276*, 44669–44676. https://doi.org/10.1074/jbc.M107179200.
37. Nern, A., Pfeiffer, B.D., and Rubin, G.M. (2015). Optimized tools for multicolor stochastic labeling reveal diverse stereotyped cell arrangements in the fly visual system. Proc. Natl. Acad. Sci. USA *112*, E2967–E2976. https://doi.org/10.1073/pnas.1506763112.
38. Diao, F., Ironfield, H., Luan, H., Diao, F., Shropshire, W.C., Ewer, J., Marr, E., Potter, C.J., Landgraf, M., and White, B.H. (2015). Plug-and-play genetic access to drosophila cell types using exchangeable exon cassettes. Cell Rep. *10*, 1410–1421. https://doi.org/10.1016/j.celrep.2015.01.059.
39. Lee, P.T., Zirin, J., Kanca, O., Lin, W.W., Schulze, K.L., Li-Kroeger, D., Tao, R., Devereaux, C., Hu, Y., Chung, V., et al. (2018). A gene-specific T2A-GAL4 library for Drosophila. Elife *7*, e35574. https://doi.org/10.7554/eLife.35574.
40. Zhu, S., Chiang, A.S., and Lee, T. (2003). Development of the Drosophila mushroom bodies: elaboration, remodeling and spatial organization of dendrites in the calyx. Development *130*, 2603–2610. https://doi.org/10.1242/dev.00466.
41. Caggese, C., Barsanti, P., Viggiano, L., Bozzetti, M.P., and Caizzi, R. (1994). Genetic, molecular and developmental analysis of the glutamine synthetase isozymes of Drosophila melanogaster. Genetica *94*, 275–281. https://doi.org/10.1007/bf01443441.
42. Thimgan, M.S., Berg, J.S., and Stuart, A.E. (2006). Comparative sequence analysis and tissue localization of members of the SLC6 family of transporters in adult Drosophila melanogaster. J. Exp. Biol. *209*, 3383–3404. https://doi.org/10.1242/jeb.02328.
43. Chaturvedi, R., Stork, T., Yuan, C., Freeman, M.R., and Emery, P. (2022). Astrocytic GABA transporter controls sleep by modulating GABAergic signaling in Drosophila circadian neurons. Curr. Biol. *32*, 1895–1908.e5. https://doi.org/10.1016/j.cub.2022.02.066.
44. Michel, C.I., Kraft, R., and Restifo, L.L. (2004). Defective neuronal development in the mushroom bodies of Drosophila fragile X mental retardation 1 mutants. J. Neurosci. *24*, 5798–5809. https://doi.org/10.1523/JNEUROSCI.1102-04.2004.
45. Eins, S., Spoerri, P.E., and Heyder, E. (1983). GABA or sodium-bromide-induced plasticity of neurites of mouse neuroblastoma cells in culture. A quantitative study. Cell Tissue Res. *229*, 457–460. https://doi.org/10.1007/bf00214987.
46. Barbin, G., Pollard, H., Gaïarsa, J.L., and Ben-Ari, Y. (1993). Involvement of GABAA receptors in the outgrowth of cultured hippocampal neurons. Neurosci. Lett. *152*, 150–154. https://doi.org/10.1016/0304-3940(93)90505-f.
47. Sinakevitch, I., Grau, Y., Strausfeld, N.J., and Birman, S. (2010). Dynamics of glutamatergic signaling in the mushroom body of young adult Drosophila. Neural Dev. *5*, 10. https://doi.org/10.1186/1749-8104-5-10.
48. Enell, L.E., Kapan, N., Söderberg, J.A.E., Kahsai, L., and Nässel, D.R. (2010). Insulin signaling, lifespan and stress resistance are modulated by metabotropic GABA receptors on insulin producing cells in the brain of Drosophila. PLoS One *5*, e15780. https://doi.org/10.1371/journal.pone.0015780.
49. Cao, J., Ni, J., Ma, W., Shiu, V., Milla, L.A., Park, S., Spletter, M.L., Tang, S., Zhang, J., Wei, X., et al. (2014). Insight into insulin secretion from transcriptome and genetic analysis of insulin-producing cells of Drosophila. Genetics *197*, 175–192. https://doi.org/10.1534/genetics.113.160663.
50. Bear, M.F., Huber, K.M., and Warren, S.T. (2004). The mGluR theory of fragile X mental retardation. Trends Neurosci. *27*, 370–377. https://doi.org/10.1016/j.tins.2004.04.009.
51. Chang, S., Bray, S.M., Li, Z., Zarnescu, D.C., He, C., Jin, P., and Warren, S.T. (2008). Identification of small molecules rescuing fragile X syndrome phenotypes in Drosophila. Nat. Chem. Biol. *4*, 256–263. https://doi.org/10.1038/nchembio.78.
52. MacArthur, I.C., and Dawlaty, M.M. (2021). TET Enzymes and 5-Hydroxymethylcytosine in Neural Progenitor Cell Biology and Neurodevelopment. Front. Cell Dev. Biol. *9*, 645335. https://doi.org/10.3389/fcell.2021.645335.
53. Weng, Y.L., An, R., Cassin, J., Joseph, J., Mi, R., Wang, C., Zhong, C., Jin, S.G., Pfeifer, G.P., Bellacosa, A., et al. (2017). An Intrinsic Epigenetic Barrier for Functional Axon Regeneration. Neuron *94*, 337–346.e6. https://doi.org/10.1016/j.neuron.2017.03.034.
54. Ismail, J.N., Badini, S., Frey, F., Abou-Kheir, W., and Shirinian, M. (2019). Drosophila Tet Is Expressed in Midline Glia and Is Required for Proper Axonal Development. Front. Cell. Neurosci. *13*, 252. https://doi.org/10.3389/fncel.2019.00252.
55. Frey, F., Sandakly, J., Ghannam, M., Doueiry, C., Hugosson, F., Berlandi, J., Ismail, J.N., Gayden, T., Hasselblatt, M., Jabado, N., and Shirinian, M. (2022). Drosophila Tet Is Required for Maintaining Glial Homeostasis

in Developing and Adult Fly Brains. eNeuro *9*. https://doi.org/10.1523/eneuro.0418-21.2022.

56. Temme, C., Zhang, L., Kremmer, E., Ihling, C., Chartier, A., Sinz, A., Simonelig, M., and Wahle, E. (2010). Subunits of the Drosophila CCR4-NOT complex and their roles in mRNA deadenylation. RNA *16*, 1356–1370. https://doi.org/10.1261/rna.2145110.
57. Collart, M.A. (2016). The Ccr4-Not complex is a key regulator of eukaryotic gene expression. Wiley Interdiscip. Rev. RNA *7*, 438–454. https://doi.org/10.1002/wrna.1332.
58. Tan, W., Schauder, C., Naryshkina, T., Minakhina, S., and Steward, R. (2016). Zfrp8 forms a complex with fragile-X mental retardation protein and regulates its localization and function. Dev. Biol. *410*, 202–212. https://doi.org/10.1016/j.ydbio.2015.12.008.
59. Rulifson, E.J., Kim, S.K., and Nusse, R. (2002). Ablation of insulin-producing neurons in flies: growth and diabetic phenotypes. Science *296*, 1118–1120. https://doi.org/10.1126/science.1070058.
60. Nässel, D.R. (2012). Insulin-producing cells and their regulation in physiology and behavior of Drosophila. Can. J. Zool. *90*, 476–488. https://doi.org/10.1139/z2012-009.
61. Barber, A.F., Erion, R., Holmes, T.C., and Sehgal, A. (2016). Circadian and feeding cues integrate to drive rhythms of physiology in Drosophila insulin-producing cells. Genes Dev. *30*, 2596–2606. https://doi.org/10.1101/gad.288258.116.
62. Nässel, D.R., Kubrak, O.I., Liu, Y., Luo, J., and Lushchak, O.V. (2013). Factors that regulate insulin producing cells and their output in Drosophila. Front. Physiol. *4*, 252. https://doi.org/10.3389/fphys.2013.00252.
63. Monyak, R.E., Emerson, D., Schoenfeld, B.P., Zheng, X., Chambers, D.B., Rosenfelt, C., Langer, S., Hinchey, P., Choi, C.H., McDonald, T.V., et al. (2017). Insulin signaling misregulation underlies circadian and cognitive deficits in a Drosophila fragile X model. Mol. Psychiatry *22*, 1140–1148. https://doi.org/10.1038/mp.2016.51.
64. Featherstone, D.E., Rushton, E., and Broadie, K. (2002). Developmental regulation of glutamate receptor field size by nonvesicular glutamate release. Nat. Neurosci. *5*, 141–146. https://doi.org/10.1038/nn789.
65. Martinez-Hernandez, A., Bell, K.P., and Norenberg, M.D. (1977). Glutamine synthetase: glial localization in brain. Science *195*, 1356–1358. https://doi.org/10.1126/science.14400.
66. Feldmann, N., del Rio, R.M., Gjinovci, A., Tamarit-Rodriguez, J., Wollheim, C.B., and Wiederkehr, A. (2011). Reduction of plasma membrane glutamate transport potentiates insulin but not glucagon secretion in pancreatic islet cells. Mol. Cell. Endocrinol. *338*, 46–57. https://doi.org/10.1016/j.mce.2011.02.019.
67. Anderson, C.M., Bridges, R.J., Chamberlin, A.R., Shimamoto, K., Yasuda-Kamatani, Y., and Swanson, R.A. (2001). Differing effects of substrate and non-substrate transport inhibitors on glutamate uptake reversal. J. Neurochem. *79*, 1207–1216. https://doi.org/10.1046/j.1471-4159.2001.00668.x.
68. Prickett, T.D., and Samuels, Y. (2012). Molecular pathways: dysregulated glutamatergic signaling pathways in cancer. Clin. Cancer Res. *18*, 4240–4246. https://doi.org/10.1158/1078-0432.Ccr-11-1217.
69. Miladinovic, T., Nashed, M.G., and Singh, G. (2015). Overview of Glutamatergic Dysregulation in Central Pathologies. Biomolecules *5*, 3112–3141. https://doi.org/10.3390/biom5043112.
70. Montanari, M., Martella, G., Bonsi, P., and Meringolo, M. (2022). Autism Spectrum Disorder: Focus on Glutamatergic Neurotransmission. Int. J. Mol. Sci. *23*, 3861. https://doi.org/10.3390/ijms23073861.
71. Géminard, C., Rulifson, E.J., and Léopold, P. (2009). Remote control of insulin secretion by fat cells in Drosophila. Cell Metab. *10*, 199–207. https://doi.org/10.1016/j.cmet.2009.08.002.
72. Markstein, M., Pitsouli, C., Villalta, C., Celniker, S.E., and Perrimon, N. (2008). Exploiting position effects and the gypsy retrovirus insulator to engineer precisely expressed transgenes. Nat. Genet. *40*, 476–483. https://doi.org/10.1038/ng.101.
73. Schindelin, J., Arganda-Carreras, I., Frise, E., Kaynig, V., Longair, M., Pietzsch, T., Preibisch, S., Rueden, C., Saalfeld, S., Schmid, B., et al. (2012). Fiji: an open-source platform for biological-image analysis. Nat. Methods *9*, 676–682. https://doi.org/10.1038/nmeth.2019.
74. Bolger, A.M., Lohse, M., and Usadel, B. (2014). Trimmomatic: a flexible trimmer for Illumina sequence data. Bioinformatics *30*, 2114–2120. https://doi.org/10.1093/bioinformatics/btu170.
75. Kim, D., Paggi, J.M., Park, C., Bennett, C., and Salzberg, S.L. (2019). Graph-based genome alignment and genotyping with HISAT2 and HISAT-genotype. Nat. Biotechnol. *37*, 907–915. https://doi.org/10.1038/s41587-019-0201-4.
76. Li, H., Handsaker, B., Wysoker, A., Fennell, T., Ruan, J., Homer, N., Marth, G., Abecasis, G., and Durbin, R.; 1000 Genome Project Data Processing Subgroup (2009). The Sequence Alignment/Map format and SAMtools. Bioinformatics *25*, 2078–2079. https://doi.org/10.1093/bioinformatics/btp352.
77. Liao, Y., Smyth, G.K., and Shi, W. (2019). The R package Rsubread is easier, faster, cheaper and better for alignment and quantification of RNA sequencing reads. Nucleic Acids Res. *47*, e47. https://doi.org/10.1093/nar/gkz114.
78. Love, M.I., Huber, W., and Anders, S. (2014). Moderated estimation of fold change and dispersion for RNA-seq data with DESeq2. Genome Biol. *15*, 550. https://doi.org/10.1186/s13059-014-0550-8.
79. Blighe, K., Rana, S., and Lewis, M. (2023). EnhancedVolcano: Publication-ready volcano plots with enhanced colouring and labeling. https://doi.org/10.18129/B9.bioc.EnhancedVolcano.
80. Strauss, A.L., Kawasaki, F., and Ordway, R.W. (2015). A Distinct Perisynaptic Glial Cell Type Forms Tripartite Neuromuscular Synapses in the Drosophila Adult. PLoS One *10*, e0129957. https://doi.org/10.1371/journal.pone.0129957.
81. Viswanathan, S., Williams, M.E., Bloss, E.B., Stasevich, T.J., Speer, C.M., Nern, A., Pfeiffer, B.D., Hooks, B.M., Li, W.P., English, B.P., et al. (2015). High-performance probes for light and electron microscopy. Nat. Methods *12*, 568–576. https://doi.org/10.1038/nmeth.3365.
82. Tran, H.H., Dang, S.N.A., Nguyen, T.T., Huynh, A.M., Dao, L.M., Kamei, K., Yamaguchi, M., and Dang, T.T.P. (2018). Drosophila Ubiquitin C-Terminal Hydrolase Knockdown Model of Parkinson's Disease. Sci. Rep. *8*, 4468. https://doi.org/10.1038/s41598-018-22804-w.
83. Livak, K.J., and Schmittgen, T.D. (2001). Analysis of relative gene expression data using real-time quantitative PCR and the 2(-Delta Delta C(T)) Method. Methods *25*, 402–408. https://doi.org/10.1006/meth.2001.1262.

STAR★METHODS

KEY RESOURCES TABLE

REAGENT or RESOURCE	SOURCE	IDENTIFIER
Antibodies		
Fas2	Developmental Studies Hybridoma Bank	Cat#1D4; RRID: AB_528235
GFP	Invitrogen	Cat#A-11122; RRID: AB_221569
Glutamine synthetase (GS)	Millipore-Sigma	Cat#MAB302; RRID: AB_2110656
HA	Invitrogen	Cat#MA5-27915; RRID: AB_2744968
β-Tubulin	BioLegend	Cat#903401; RRID: AB_2565030
Goat Anti-Mouse IgG, Cy3	Jackson ImmunoResearch	Cat#115-165-003; RRID: AB_2338680
Donkey Anti-Rabbit IgG, Cy5	Jackson ImmunoResearch	Cat#711-175-152; RRID: AB_2340607
Goat anti-Mouse IgG, Alexa Fluor 488	Invitrogen	Cat#A-11001; RRID: AB_2534069
Goat anti-Mouse IgG, IRDye 800CW	LI-COR	Cat#926–32210; RRID: AB_2687825
Dilp2	Géminard et al.[71]	N/A
Biological samples		
Drosophila brains	This study	N/A
Chemicals, peptides, and recombinant proteins		
2-Methyl-6-(phenylethynyl)pyridine (MPEP)	Enzo	Cat#ALX-550-368-M005
L-Glutamic acid monosodium salt hydrate	Sigma-Aldrich	Cat#G5889-100G
Schneider's Drosophila Medium	ThermoFisher	Cat#21720024
Vectashield mounting medium	Vector Laboratories	Cat#H-1000-10
Normal goat serum	Vector Laboratories	Cat#S-1000
Formaldehyde	Fisher Scientific	Cat#F79-500
RNase-Free DNase	QIAGEN	Cat#79254
Phusion Hot Start II HF	Thermo Scientific	Cat#F565S
RIPA buffer	Thermo Scientific	Cat#89900
Protease Inhibitor Cocktail	Roche	Cat#5892791001
Critical commercial assays		
RNeasy Plus Universal Kit	QIAGEN	Cat#73404
NEBNext Ultra Directional RNA Library Prep Kit for Illumina	New England Biolabs	Cat#E7530
RNA Nano 6000 Kit	Agilent Technologies	Cat#5067-1511
AMPure XP	Beckman Coulter	Cat#A63882
PE Cluster Kit cBot-HS	Illumina	Cat#PE-401-3001
NovaSeq 6000 Reagent Kits	Illunina	Cat#20028312
MMLV High-Performance Reverse Transcriptase Kit	Biosearch Technologies	Cat#RT80125K
PowerUp SYBR Green Master Mix	Applied Biosystems	Cat#A25741
NEBuilder HiFi DNA Assembly Cloning Kit	New England Biolabs	Cat#E5520S
Deposited data		
RNA-seq raw and analyzed data	This study	GEO: GSE231534
Code for RNA-seq data analysis	This study	https://doi.org/10.5281/zenodo.10864320
Experimental models: Organisms/strains		
Tet^{AXXC}	This study	N/A

(*Continued on next page*)

Continued

REAGENT or RESOURCE	SOURCE	IDENTIFIER
Tet^{YRA}	This study	N/A
UAS-Gs2	This study	N/A
nos-Cas9	Bloomington Drosophila Stock Center	BDSC:54591
3xP3-ECFP, alpha-tub-piggyBacK10/TM6C, Sb^1	Bloomington Drosophila Stock Center	BDSC:32072
UAS-GFP::CD8, 201Y-GAL4	Bloomington Drosophila Stock Center	BDSC:64296
Tet-T2A-GAL4-pA	Bloomington Drosophila Stock Center	BDSC:76666
MCFO-2	Bloomington Drosophila Stock Center	BDSC:64086
Act5C-Cas9	Bloomington Drosophila Stock Center	BDSC:54590
Gs2 TKO	Bloomington Drosophila Stock Center	BDSC:76492
Gs2 RNAi	Bloomington Drosophila Stock Center	BDSC:92838
Gat RNAi	Bloomington Drosophila Stock Center	BDSC:29422
Robo2 RNAi #27317	Bloomington Drosophila Stock Center	BDSC:27317
Robo2 RNAi #34589	Bloomington Drosophila Stock Center	BDSC:34589
mCherry RNAi	Bloomington Drosophila Stock Center	BDSC:35785
tubP-GAL80ts	Bloomington Drosophila Stock Center	BDSC:7017
UAS-Dcr2	Bloomington Drosophila Stock Center	BDSC:24651
Tet RNAi #36188	Vienna Drosophila Resource Center	VDRC:36188 (GD#14330)
Tet RNAi #110549	Vienna Drosophila Resource Center	VDRC:110549 (KK#108964)
Gat RNAi	Vienna Drosophila Resource Center	VDRC:106638 (KK#107895)
y^1 w^{67c23}; PCaryPattP40	Markstein et al.[72]	N/A
Dilp2-GAL4	Rulifson et al.[59]	N/A
$Fmr1^3$	Dockendorff et al.[25]	N/A
Oligonucleotides		
sgRNA and primer sequences used for CRISPR/Cas9 and HDR-mediated Tet mutation, see Table S1.	This study	N/A
Primers used for RT-qPCR, see Table S2.	This study	N/A
Primers used for UAS-Gs2 stock generation, see Table S3.	This study	N/A
Recombinant DNA		
pU6-BbsI-chiRNA	Gratz et al.[35]	Addgene Plasmid #45946
pScarlessHD-DsRed	Kate O'Connor-Giles	Addgene Plasmid #64703
Gs2 DGRC clone LP04559	Drosophila Genomics Resource Center	DGRC#1337593
pUASTattB	Drosophila Genomics Resource Center	DGRC#1419
Software and algorithms		
Image Studio Lite	Li-COR	https://www.licor.com/bio/image-studio/
Fiji	Schindelin et al.[73]	https://imagej.net/software/fiji/
Huygens Confocal Deconvolution	Scientific Volume Imaging	https://svi.nl/Huygens-Confocal-Software
LAS X Lightning Deconvolution	Leica Microsystem	https://www.leica-microsystems.com/products/microscope-software/p/leica-las-x-ls/
GraphPad Prism	GraphPad Software	https://www.graphpad.com/
Trimmomatic	Bolger et al.[74]	http://www.usadellab.org/cms/?page=trimmomatic
HISAT2	Kim et al.[75]	https://daehwankimlab.github.io/hisat2/
Samtools	Li et al.[76]	https://www.htslib.org/

(*Continued on next page*)

Continued

REAGENT or RESOURCE	SOURCE	IDENTIFIER
FeatureCounts	Liao et al.[77]	https://subread.sourceforge.net/featureCounts.html
DESeq2	Love et al.[78]	https://bioconductor.org/packages/release/bioc/html/DESeq2.html
EnhancedVolcano	Blighe et al.[79]	https://bioconductor.org/packages/release/bioc/html/EnhancedVolcano.html

RESOURCE AVAILABILITY

Lead contact

Further information and requests for resources, reagents, and source data should be directed to and will be fulfilled by the lead contact, Ruth Steward (steward@waksman.rutgers.edu).

Materials availability

Materials generated in this study are available upon request from the lead contact.

Data and code availability

- RNA-seq data have been deposited at GEO and are publicly available as of the date of publication. The accession number is listed in the key resources table. Microscopy data reported in this paper will be shared by the lead contact upon request.
- All original code for RNA-seq data analysis has been deposited at Zenodo and is publicly available as of the date of publication. DOI is listed in the key resources table.
- Any additional information required to reanalyze the data reported in this study is available from the lead contact upon request.

EXPERIMENTAL MODELS AND STUDY PARTICIPANT DETAILS

Fly stocks

Fly stocks were cultured on standard food medium at 25°C. Tet^{AXXC}, $Tet^{YRA,}$ and USA-Gs2 fly strains were generated in this study. The following stocks were obtained from Bloomington Drosophila Stock Center (BDSC): nos-Cas9 (#54591), 3xP3-ECFP, alpha-tub-piggyBacK10/TM6C, Sb1 (#32072), UAS-mCD8:GFP, 201Y-GAL4 driver (#64296),[28] enhancer trap Tet-T2A-GAL4-pA (#76666),[39] multicolor flip-out stock MCFO-2 (#64086),[37] Act5C-Cas9 (#54590), Gs2 TKO for Gs2 CRISPR/Cas9 mutagenesis (#76492), Gs2 RNAi (#92838),[80] Gat RNAi (#29422), mCherry RNAi (#35785), tubP-$GAL80^{ts}$ (#7017), and UAS-Dcr2 (#24651). Tet and Gat RNAi lines were obtained from Vienna Drosophila Resource Center (VDRC, GD#14330, KK#108964, and KK#107895). y^1 w^{67c23}; PCaryPattP40 was obtained from Dr. Norbert Perrimon.[72] Dilp2-GAL4 was originally obtained from Dr. Eric Rulifson (University of California, San Francisco).[59] $Fmr1^3$ mutant was kindly provided by Dr. Thomas A. Jongens (University of Pennsylvania).[25] All the *Drosophila* stocks in this paper are listed in the key resources table. This study was conducted in the mixed-sex *Drosophila* population with 50% males and females. The age and developmental stage for each experiment are provided in the method details.

METHOD DETAILS

Generating targeted Tet^{AXXC} and Tet^{YRA} mutants using CRISPR/Cas9 and HDR

The Tet^{AXXC} mutant was generated using the scarless gene editing approach which is mediated by CRISPR/Cas9 cut and homologous directed repair (HDR) of the designed DNA template harboring targeted mutations.[33–35] Two gRNAs (gRNA1 and gRNA2) were designed to bind to both sides of the CXXC zinc finger domain flanking regions to guide the Cas9 cuts. These gRNAs were synthesized (IDT, USA) and cloned into the pU6-BbsI-chiRNA expression vector (Addgene #45946).[35] The two homology arms were generated by PCR from the nos-Cas9 stock (BDSC # 54591) genomic DNA. The PCR was done using gene-specific and mutated primers to generate one wild-type homology arm and one mutated homology arm with at least 1000 bp overlap with the genomic DNA flanking the cut site. The homology arms were cloned into the pScarlessHD-DsRed donor vector (Addgene # 64703, gift from Kate O'Connor-Giles). The mixture of these vectors was injected into the nos-Cas9 stock and screened for the dsRed marker. dsRed positive lines were genetically crossed to remove the non-Cas9 chromosome. Then, these lines were crossed to a piggyBac recombinase stock 3xP3-ECFP, alpha-tub-piggyBacK10/TM6C, Sb^1 (BDSC # 32072) to excise the dsRed marker. The mutant stocks were validated by PCR and Sanger sequencing. The Tet^{YRA} mutant was generated using the same method. The sequences for sgRNAs and primers to generate homology arms are listed in Table S1.

Lethality

Seven pairs of flies were kept on the standard medium at 25°C for 24 h egg laying. Then the flies were transferred five more times to new vials at 24-h intervals. The lethality of the Tet^{null} mutant was previously known[3,6]; thus, the flies were kept after adult eclosion for lethality assessment. The eclosed flies were removed from the vials every day and the number of total and lethal pupae was counted after all the viable flies had eclosed (~20 days after egg laying at 25°C). The percentage of lethality was calculated based on the number of lethal pupae out of the total number of pupae observed.

Conditional knockdown using temperature shift $GAL80^{ts}$

The driver 201Y-GAL4 was crossed with *Tet RNAi (*GD#14330*); GAL80ts* or *mCherry RNAi; GAL80ts* to generate Tet knockdown $GAL80^{ts}$ or mCherry RNAi control $GAL80^{ts}$. The crosses and progenies were kept at 18°C or 29°C following the temperature shift scheme detailed in (Figure 2B). Five to ten days old adult brains were dissected and stained to calculate the percentage of β fusion phenotype on each condition.

Simultaneously knockdown and visualizing growing axons using Tet-T2A-GAL4

The Tet enhancer trap line Tet-T2A-GAL4-pA[39] was used as Tet-T2A-GAL4 driver for Tet knockdown in Tet-expressing cells in the pupal brain and labeling of cell bodies and axons in the same cells. The knockdown can be accomplished because Tet-T2A-GAL4-pA was inserted between exons 5 and 6 but the RNAi (stock #110549 VDRC, construct KK#108964) targets sequences in exon 8 (Figure S2A). The knockdown efficiency was assessed in larval brains by RT-qPCR using the ubiquitous driver da-GAL4 (Figure S2B). The poly(A) (pA) signal will trigger the transcriptional termination to ensure the RNAi will not bind and degrade the transcript containing the GAL4 coding sequence. To label axons with high resolution, we employed the MCFO2 stock which can express membrane tethered smGdPs (spaghetti monster Green darkened Proteins) under the control of both GAL4/UAS and the heat shock FLP/FRT inducible systems.[37] smGdP is a darkened chromophore Green Protein fused with multiple copies of epitope tag (e.g., HA, V5, OLLAS, FLAG, and Myc) and a myristoylation for better visualization of small axons and dendrites.[81] The Tet RNAi stock (KK#108964) or mCherry RNAi were crossed to the flip-out stock MCFO-2 to generate *UAS-Tet RNAi; MCF O -2* or *UAS-mCherry RNAi; MCF O -2* stocks. Then, Tet-GAL4 was crossed to the *UAS-Tet RNAi; MCF O -2* for Tet knockdown and labeling axons of Tet expressing neurons, or *UAS-mCherry RNAi; MCF O -2* for the control. The crosses were kept at 25°C to produce white pupae. Then, white pupae were collected and placed on the wall of the *Drosophila* glass vials. The vials were heat shocked for 3 min at 37°C in a water bath, then transferred to a 25°C incubator and grown for 21 h. Then, pupal brains were dissected and stained to visualize the growing MB axons.

Brain dissection, immunostaining and imaging

Brain dissection and immunostaining were performed based on the previous method[82] with the following modifications. Adult brains of males and females (5–10 days old) were dissected in cold 1X phosphate-buffered saline (PBS) and fixed in 4% formaldehyde at 25°C for 20 min on a slow rotator (7 rpm). Pupal brains were dissected in cold PBS, and then immediately transferred to a cold fixation solution containing 4% formaldehyde diluted in Schneider's *Drosophila* Medium (Gibco # 21720024) on ice. The pupal brains can be kept in the cold fixation solution for a maximum of 1 h. Then the pupal brains were fixed at 25°C for 45 min on a slow rotator (7 rpm). After fixing, brains were quickly washed with 0.3% PBS-T (0.3% Triton X-100 in 1X PBS) one time, then three washes with 0.3% PBS-T, 20 min each. The brains were blocked in blocking solution (0.15% PBS-T containing 10% normal goat serum) at 25°C for 20 min. The brains were then incubated with the following primary antibodies diluted in blocking solution: mouse anti-Fasciclin II antibody (Fas2, DSHB #1D4, deposited by Corey Goodman, 1:50), rat anti-Dilp2 antibody (a gift from Pierre Leopold, Institut Curie, 1:400),[71] rabbit anti-GFP antibody (Invitrogen #A-11122, 1:1000), mouse anti-glutamine synthetase (GS) antibody, clone GS-6 (Millipore-Sigma #MAB302, 1:1000) at 4°C overnight or rabbit anti-HA antibody (Invitrogen #MA5-27915, 1:1000) at 4°C over two nights. After primary antibody incubation, the brains were washed with 0.3% PBS-T, 3 times for 20 min each. Then, brains were incubated with secondary antibodies conjugated with Cy3 (Jackson ImmunoResearch #115-165-003, 1:400), Cy5 (Jackson ImmunoResearch #711-175-152, 1:400), or Alexa 488 (Invitrogen # A-11001, 1:400) at 4°C overnight or over two nights (Figures 2E–2L). Brains were washed 3 times, 20 min each with 0.3% PBS-T followed by 2 quick washes with 1X PBS. The brains were mounted in Vectashield mounting medium (Vector Laboratories # H-1000-10) in SecureSeal imaging spacers (Electron Microscopy Sciences #70327-9S). Brains were imaged using Leica SP8 confocal microscope (Leica Microsystem) and deconvoluted using either Lightning Deconvolution (Leica Microsystem, USA) or Huygens Confocal Deconvolution (Scientific Volume Imaging, Netherlands). The images were processed using Fiji.[73]

Total RNA isolation

Pupal brains were dissected in PBS and immediately frozen on dry ice. Totally, 30 brains per genotype were collected at 24h APF (After Puparium Formation). Three independent biological replicates per genotype were used for RNA isolation. Total RNA was isolated using RNeasy Plus Universal Kit (QIAGEN, USA) following the manufacturer's instructions including DNase I treatment using RNase-Free DNase Set and on-column protocol (QIAGEN, USA). The isolated total RNAs were aliquoted for both RNA-seq and qRT-PCR.

Quantitative reverse transcription PCR (RT-qPCR)

One microgram of total RNA from wild-type, Tet, and Fmr1 mutants was reserve transcribed to produce cDNAs using MMLV High-Performance Reverse Transcriptase Kit (Biosearch Technologies #RT80125K) and oligo(dT) primers (IDT, USA). The cDNAs were used for

real-time quantitative PCR using gene-specific primers with Rpl32 as the internal reference control (Table S2) and PowerUp SYBR Green Master Mix (Applied Biosystems #A25741) with the StepOnePlus Real-Time PCR System (Applied Biosystems, USA). The relative quantification (RQ) for the expression of each gene was calculated using the comparative Ct method.[83]

RNA-seq library generation

Library preparation and sequencing were performed at Novogene. One microgram of total RNA was used as input for library preparation. Prior to library preparation, total RNA quality was validated for the following parameters: degradation and contamination using 1% agarose gel electrophoresis, purity by NanoPhotometer spectrophotometer (IMPLEN, USA), and integrity using Bioanalyzer 2100 and RNA Nano 6000 Kit (Agilent Technologies, USA). Sequencing libraries were generated using NEBNext Ultra Directional RNA Library Prep Kit for Illumina (NEB, USA) following the manufacturer's instruction. mRNA was purified from total RNA using oligo dT magnetic beads. Purified mRNAs were fragmented by divalent cations. First-strand cDNA synthesis was done using random hexamer and M-MuLV RT (RNase H-). The dUTP method was used to synthesize the second strand and to generate a strand-specific library. 3′ A overhangs were cleaved by exonuclease, DNA fragments were ligated with NEBNext hairpin loop adapter to prepare for hybridization. AMPure XP system (Beckman Coulter, USA) was used for 150–200 bp size selection. The size selected and purified products were treated with USER Enzyme to open up the NEBNext adapter. Then, PCR was performed with Phusion High-Fidelity DNA polymerase using Universal PCR primers and Index (X) prime. PCR products were purified using the AMPure XP system and quality was assessed by Agilent Bioanalyzer 2100. Clustering was done using cBot Cluster System using PE Cluster Kit cBot-HS (Illumina, USA) according to the manufacturer's recommendation. Sequencing was performed on Illumina Novaseq 6000 (Illumina, USA) to generate paired-end reads.

RNA-seq data analysis

Raw reads were filtered and trimmed by Trimmomatic 0.39.[74] Then, the filtered reads were mapped to Ensembl *Drosophila melanogaster* genome assembly BDGP6.22 using HISAT2.[75] The mapping SAM files were converted to BAM using Samtools.[76] The number of reads mapped to the individual gene is counted by featureCounts.[77] Differential gene expression analysis was done by DESeq2.[78] Results were visualized by the Bioconductor package EnhancedVolcano.[79]

Western blot

Thirty L3 instar larval brains from Act5C-GAL4 driving Gs2 CRISPR/Cas9 mutagenesis or Act5C-GAL4 wild-type control were dissected and immediately frozen on dry ice. Total protein was isolated from these brains using RIPA buffer (25 mM Tris HCl pH 7.6, 150 mM NaCl, 1% NP-40, 1% sodium deoxycholate, 0.1% SDS; Thermo Scientific #89900) supplemented with 1X Protease Inhibitor Cocktail (Roche # 5892791001) and 25ug of the total protein was loaded into each well. Glutamine synthetase antibody, clone GS-6 (Millipore-Sigma #MAB302) was used at 1: 2000 dilution and beta-tubulin antibody, clone TU27 (BioLegend # 903401) was used at 1: 1000 dilution. The western blot signals were detected using anti-mouse IRDye 800CW Infrared Dyes conjugated secondary antibody in the LICOR Odyssey CLx imaging system. Signals were quantified using LICOR Image Studio Lite software.

MPEP and glutamate treatment

MPEP and glutamate treatment were conducted as described in previous studies[21,51] with the following modifications. Wild type and Tet^{AXXC} mutant flies were grown on the standard medium at 25°C to early third instar larva. Then, sixty larvae were collected and transferred to a vial containing either MPEP- or glutamate-supplemented medium at 100 μM, or water-supplemented medium as diluent control. Twelve hours after transferring, larvae that were not in the medium were eliminated to ensure all larvae consumed the supplemented medium for at least 12 h. This allows the larvae to uptake MPEP or glutamate before they begin to pupate and stop eating. The larvae were left in the vials to grow into adults. After eclosion adults were transferred to the standard medium. Five to ten-day-old adult brains were dissected and immunostained to quantify the percentage of MB β lobe fusion per each condition.

Generating UAS-Gs2 transgene stocks

Gs2 cDNA was obtained from *Drosophila* Genomics Resource Center (DGRC) clone LP04559 (DGRC #1337593). The coding region was amplified by Phusion Hot Start II HF (Thermo Scientific #F565S) using gene-specific primers with homology arms designed for DNA Assembly (Table S3). The amplicon was cloned to the pUASTattB expression vector (DGRC #1419, deposited by Bischof and Basler) at the EcoRI restriction site by NEBuilder HiFi DNA Assembly Cloning Kit (NEB #E5520S). The pUASTattB-Gs2 vector was injected to $y^1\ w^{67c23}$; *PCaryPattP40* stock[72] by the BestGene company to insert the UAS-Gs2 construct to attP40 landing site on the second chromosome. *UAS-Gs2* stocks were validated by genomic PCR and Sanger sequencing.

UAS-GS2 flies were crossed with Tet^{AXXC} and $Fmr1^3$ mutants to generate *UAS-Gs2;* Tet^{AXXC}/*TM6B* Tb^1 and *UAS-Gs2;* $Fmr1^3$/*TM6B* Tb^1. The Tet^{AXXC} and $Fmr1^3$ mutants were also crossed with the *Dilp2-GAL4* driver to generate *Dilp2-GAL4;* Tet^{AXXC}/*TM6* Sb^1 and *Dilp2-GAL4;* $Fmr1^3$/*TM6* Sb^1. Flies were crossed to generate rescued stocks and respective controls. The progenies were collected after eclosion, separated to eliminate balancers, transferred to fresh medium, and dissected at five to ten days old for MB β lobe immunostaining and quantification.

QUANTIFICATION AND STATISTICAL ANALYSIS

MB axon guidance phenotype was quantified based on the previously described method[21,44,51] with the following modifications. The animals were randomly selected for brain dissection and staining, and the phenotype was scored based on anti-Fas2 staining. The total number of brains was recorded at the end of imaging and presented in figure legends. The phenotype was scored as 1 if the brain showed any β lobe fusion in the mushroom body or 0 if the brain had no fusion similar to what is observed in the wild-type brain. The phenotypic assessment was done by investigators who were blind to the genotype. The percentage of brains that had β lobe fusion was calculated based on the sum of scores and the total number of brains. The statistical analyses were done using Chi-square tests, GraphPad Prism (GraphPad Software, USA). The significant difference was indicated by $*p < 0.05$, $**p < 0.01$, $***p < 0.001$, $****p < 0.0001$, ns for non-significant. The data are represented as percentages or mean ± SD as defined in each figure legend.